REFERENCES

1. Williams, C. S., and DuBois, R. N. (1996) Prostaglandin endoperoxide synthase: why two isoforms? *Am. J. Physiol.* 270, G393–G400
2. Arslan, A., and Zingg, H. H. (1996) Regulation of COX-2 gene expression in rat uterus in vivo and in vitro. *Prostaglandins* 52, 463–481
3. Tanaka, Y., Takahashi, M., Kawaguchi, M., and Amano, F. (1997) Delayed release of prostaglandins from arachidonic acid and kinetic changes in prostaglandin H synthase activity on the induction of prostaglandin H synthase-2 after lipopolysaccharide-treatment of RAW264.7 macrophage-like cells. *Biol. Pharm. Bull.* 20, 322–326
4. Sheng, H., Shao, J., Washington, M. K., and DuBois, R. N. (2001) Prostaglandin E2 increases growth and motility of colorectal carcinoma cells. *J. Biol. Chem.* 276, 18075–18081
5. Ben-Av, P., Crofford, L. J., Wilder, R. L., and Hla, T. (1995) Induction of vascular endothelial growth factor expression in synovial fibroblasts by prostaglandin E and interleukin-1: a potential mechanism for inflammatory angiogenesis. *FEBS Lett.* 372, 83–87
6. Tsuji, S., Kawano, S., Tsujii, M., Michida, T., Masuda, E., Gunawan, E. S., and Hori, M. (1998) Mucosal microcirculation and angiogenesis in gastrointestinal tract. *Nippon Rinsho* 56, 2247–2252
7. Sheng, H., Shao, J., Morrow, J. D., Beauchamp, R. D., and DuBois, R. N. (1998) Modulation of apoptosis and Bcl-2 expression by prostaglandin E2 in human colon cancer cells. *Cancer Res.* 58, 362–366
8. Kakiuchi, Y., Tsuji, S., Tsujii, M., Murata, H., Kawai, N., Yasumaru, M., Kimura, A., Komori, M., Irie, T., Miyoshi, E., et al. (2002) Cyclooxygenase-2 activity altered the cell-surface carbohydrate antigens on colon cancer cells and enhanced liver metastasis. *Cancer Res.* 62, 1567–1572
9. Tsuji, S., Tsujii, M., Kawano, S., and Hori, M. (2001) Cyclooxygenase-2 upregulation as a perigenetic change in carcinogenesis. *J. Exp. Clin. Cancer Res.* 20, 117–129
10. Sano, H., Kawahito, Y., Wilder, R. L., Hashiramoto, A., Mukai, S., Asai, K., Kimura, S., Kato, H., Kondo, M., and Hla, T. (1995) Expression of cyclooxygenase-1 and -2 in human colorectal cancer. *Cancer Res.* 55, 3785–3789
11. Murata, H., Kawano, S., Tsuji, S., Tsuji, M., Sawaoka, H., Kimura, Y., Shiozaki, H., and Hori, M. (1999) Cyclooxygenase-2 overexpression enhances lymphatic invasion and metastasis in human gastric carcinoma. *Am. J. Gastroenterol.* 94, 451–455
12. Xue, Y. W., Zhang, Q. F., Zhu, Z. B., Wang, Q., and Fu, S. B. (2003) Expression of cyclooxygenase-2 and clinicopathologic features in human gastric adenocarcinoma. *World J. Gastroenterol.* 9, 250–253
13. Achiwa, H., Yatabe, Y., Hida, T., Kuroishi, T., Kozaki, K., Nakamura, S., Ogawa, M., Sugiura, T., Mitsudomi, T., and Takahashi, T. (1999) Prognostic significance of elevated cyclooxygenase 2 expression in primary, resected lung adenocarcinomas. *Clin. Cancer Res.* 5, 1001–1005
14. Richards, R. G., and Almond, G. W. (1994) Lipopolysaccharide-induced increases in porcine serum cortisol and progesterone concentrations are not mediated solely by prostaglandin F2 alpha. *Inflammation* 18, 203–214
15. Davis, B. J., Lennard, D. E., Lee, C. A., Tiano, H. F., Morham, S. G., Wetsel, W. C., and Langenbach, R. (1999) Anovulation in cyclooxygenase-2-deficient mice is restored by prostaglandin E2 and interleukin-1beta. *Endocrinology* 140, 2685–2695
16. Caivano, M., and Cohen, P. (2000) Role of mitogen-activated protein kinase cascades in mediating lipopolysaccharide-stimulated induction of cyclooxygenase-2 and IL-1 beta in RAW264 macrophages. *J. Immunol.* 164, 3018–3025
17. Kirtikara, K., Raghow, R., Laulederkind, S. J., Goorha, S., Kanekura, T., and Ballou, L. R. (2000) Transcriptional regulation of cyclooxygenase-2 in the human microvascular endothelial cell line, HMEC-1: control by the combinatorial actions of AP2, NF-IL-6 and CRE elements. *Mol. Cell. Biochem.* 203, 41–51
18. Bamba, H., Ota, S., Kato, A., Adachi, A., Itoyama, S., and Matsuzaki, F. (1999) High expression of cyclooxygenase-2 in macrophages of human colonic adenoma. *Int. J. Cancer* 83, 470–475
19. Fiebich, B. L., Mueksch, B., Boehringer, M., and Hull, M. (2000) Interleukin-1beta induces cyclooxygenase-2 and prostaglandin E(2) synthesis in human neuroblastoma cells: involvement of p38 mitogen-activated protein kinase and nuclear factor-kappaB. *J. Neurochem.* 75, 2020–2028
20. Wadleigh, D. J., and Herschman, H. R. (1999) Transcriptional regulation of the cyclooxygenase-2 gene by diverse ligands in murine osteoblasts. *Biochem. Biophys. Res. Commun.* 264, 865–870
21. Crofford, L. J., Tan, B., McCarthy, C. J., and Hla, T. (1997) Involvement of nuclear factor kappa B in the regulation of cyclooxygenase-2 expression by interleukin-1 in rheumatoid synoviocytes. *Arthritis Rheum.* 40, 226–236
22. Inoue, H., Yokoyama, C., Hara, S., Tone, Y., and Tanabe, T. (1995) Transcriptional regulation of human prostaglandin-endoperoxide synthase-2 gene by lipopolysaccharide and phorbol ester in vascular endothelial cells. Involvement of both nuclear factor for interleukin-6 expression site and cAMP response element. *J. Biol. Chem.* 270, 24965–24971
23. Yoshida, S., Ono, M., Shono, T., Izumi, H., Ishibashi, T., Suzuki, H., and Kuwano, M. (1997) Involvement of interleukin-8, vascular endothelial growth factor, and basic fibroblast growth factor in tumor necrosis factor alpha-dependent angiogenesis. *Mol. Cell. Biol.* 17, 4015–4023
24. Torisu, H., Ono, M., Kiryu, H., Furue, M., Ohmoto, Y., Nakayama, J., Nishioka, Y., Sone, S., and Kuwano, M. (2000) Macrophage infiltration correlates with tumor stage and angiogenesis in human malignant melanoma: possible involvement of TNFalpha and IL-1alpha. *Int. J. Cancer* 85, 182–188
25. Ono, M., Torisu, H., Fukushi, J., Nishie, A., and Kuwano, M. (1999) Biological implications of macrophage infiltration in human tumor angiogenesis. *Cancer Chemother. Pharmacol.* 43, S69–S71
26. Kawai, S. (1998) Drug delivery system of anti-inflammatory and anti-rheumatic drugs. *Nippon Rinsho* 56, 782–787
27. Dequeker, J., Hawkey, C., Kahan, A., Steinbruck, K., Alegre, C., Baumelou, E., Begaud, B., Isomaki, H., Littlejohn, G., and Mau, J. (1998) Improvement in gastrointestinal tolerability of the selective cyclooxygenase (COX)-2 inhibitor, meloxicam, compared with piroxicam: results of the Safety and Efficacy Large-scale Evaluation of COX-inhibiting Therapies (SELECT) trial in osteoarthritis. *Br. J. Rheumatol.* 37, 946–951
28. Reddy, B. S., and Rao, C. V. (2000) Colon cancer: a role for cyclo-oxygenase-2-specific nonsteroidal anti-inflammatory drugs. *Drugs Aging* 16, 329–334
29. Giardiello, F. M., Hamilton, S. R., Krush, A. J., Piantadosi, S., Hylind, L. M., Celano, P., Booker, S. V., Robinson, C. R., and Offerhaus, G. J. (1993) Treatment of colonic and rectal adenomas with sulindac in familial adenomatous polyposis. *N. Engl. J. Med.* 328, 1313–1316
30. Oshima, M., Dinchuk, J. E., Kargman, S. L., Oshima, H., Hancock, B., Kwong, E., Trzaskos, J. M., Evans, J. F., and Taketo, M. M. (1996) Suppression of intestinal polyposis in Apc delta-716 knockout mice by inhibition of cyclooxygenase 2 (COX-2). *Cell* 87, 803–809
31. Oshima, M., Murai, N., Kargman, S., Arguello, M., Luk, P., Kwong, E., Taketo, M. M., and Evans, J. F. (2001) Chemoprevention of intestinal polyposis in the Apcdelta716 mouse by rofecoxib, a specific cyclooxygenase-2 inhibitor. *Cancer Res.* 61, 1733–1740
32. Sawaoka, H., Tsuji, S., Tsujii, M., Gunawan, E. S., Sasaki, Y., Kawano, S., and Hori, M. (1999) Cyclooxygenase inhibitors suppress angiogenesis and reduce tumor growth in vivo. *Lab. Invest.* 79, 1469–1477
33. Masferrer, J. L., Koki, A., and Seibert, K. (1999) COX-2 inhibitors. A new class of antiangiogenic agents. *Ann. N.Y. Acad. Sci.* 889, 84–86
34. Riendeau, D., Percival, M. D., Boyce, S., Brideau, C., Charleson, S., Cromlish, W., Ethier, D., Evans, J., Falgueyret, J. P., Ford-Hutchinson, A. W., et al. (1997) Biochemical and pharmacological profile of a tetrasubstituted furanone as a highly selective COX-2 inhibitor. *Br. J. Pharmacol.* 121, 105–117
35. Wakitani, K., Nanayama, T., Masaki, M., and Matsushita, M. (1998) Profile of JTE-522 as a human cyclooxygenase-2 inhibitor. *Jpn. J. Pharmacol.* 78, 365–371
36. Hirata, A., Ogawa, S., Kometani, T., Kuwano, T., Naito, S., Kuwano, M., and Ono, M. (2002) ZD1839 (Iressa) induces

antiangiogenic effects through inhibition of epidermal growth factor receptor tyrosine kinase. *Cancer Res.* 62, 2554–2560
37. Nakao, S., Kuwano, T., Ishibashi, T., Kuwano, M., and Ono, M. (2003) Synergistic effect of TNF-α in soluble VCAM-1-induced angiogenesis through α4 integrins. *J. Immunol.* 170, 5704–5711
38. Morham, S. G., Langenbach, R., Loftin, C. D., Tiano, H. F., Vouloumanos, N., Jennette, J. C., Mahler, J. F., Kluckman, K. D., Ledford, A., Lee, C. A., et al. (1995) Prostaglandin synthase 2 gene disruption causes severe renal pathology in the mouse. *Cell* 83, 473–482
39. Ogawa, S., Yoshida, S., Ono, M., Onoue, H., Ito, Y., Ishibashi, T., Inomata, H., and Kuwano, M. (1999) Induction of macrophage inflammatory protein-1α and vascular endothelial growth factor during inflammatory neovascularization in the mouse cornea. *Angiogenesis* 3, 327–334
40. Itokawa, T., Nokihara, H., Nishioka, Y., Sone, S., Iwamoto, Y., Yamada, Y., McMahon, G., Shibuya, M., Kuwano, M., Ono, M., et al. (2002) Antiangiogenic effect by SU5416 is partly attributable to inhibition of Flt-1 receptor signaling. *Mol. Cancer Ther.* 1, 295–302
41. Voronov, E., Shouval, D. S., Krelin, Y., Cagnano, E., Benharroch, D., Iwakura, Y., Dinarello, C. A., and Apte, R. N. (2003) IL-1 is required for tumor invasiveness and angiogenesis. *Proc. Natl. Acad. Sci. USA* 100, 2645–2650
42. Yano, S., Nokihara, H., Goto, H., Ogawa, H., Kanematsu, T., Miki, T., Uehara, H., Saijo, Y., Nukiwa, T., Sone, S., et al. (2003) Multifunctional interleukin-1β promotes metastasis of human lung cancer cells in SCID mice via enhanced expression of adhesion-, invasion- and angiogenesis-related molecules. *Cancer Sci.* 94, 244–252
43. Saijo, Y., Tanaka, M., Miki, M., Suzuki, T., Maemondo, M., Hong, X., Tazawa, R., Kikuchi, T., Matsushima, K., Nukiwa, T., et al. (2002) Proinflammatory cytokine IL-1β promotes tumor growth of Lewis lung carcinoma by induction of angiogenic factors: in vivo analysis of tumor-stromal interaction. *J. Immunol.* 169, 469–475
44. Salven, P., Hattori, K., Heissig, B., and Rafii, S. (2002) Interleukin-1α promotes angiogenesis in vivo via VEGFR-2 pathway by inducing inflammatory cell VEGF synthesis and secretion. *FASEB J.* 16, 1471–1473
45. Majima, M., Hayashi, I., Muramatsu, M., Katada, J., Yamashina, S., and Katori, M. (2000) Cyclo-oxygenase-2 enhances basic fibroblast growth factor-induced angiogenesis through induction of vascular endothelial growth factor in rat sponge implants. *Br. J. Pharmacol.* 130, 641–649
46. Cheng, T., Cao, W., Wen, R., Steinberg, R. H., and LaVail, M. M. (1998) Prostaglandin E2 induces vascular endothelial growth factor and basic fibroblast growth factor mRNA expression in cultured rat Muller cells. *Invest. Ophthalmol. Vis. Sci.* 39, 581–591
47. Graeber, J. E., Glaser, B. M., Setty, B. N., Jerdan, J. A., Walenga, R. W., and Stuart, M. J. (1990) 15-Hydroxyeicosatetraenoic acid stimulates migration of human retinal microvessel endothelium in vitro and neovascularization in vivo. *Prostaglandins* 39, 665–673
48. He, H., Venema, V. J., Gu, X., Venema, R. C., Marrero, M. B., and Caldwell, R. B. (1999) Vascular endothelial growth factor signals endothelial cell production of nitric oxide and prostacyclin through flk-1/KDR activation of c-Src. *J. Biol. Chem.* 274, 25130–25135
49. Daniel, T. O., Liu, H., Morrow, J. D., Crews, B. C., and Marnett, L. J. (1999) Thromboxane A2 is a mediator of cyclooxygenase-2-dependent endothelial migration and angiogenesis. *Cancer Res.* 59, 4574–4577
50. Coussens, L. M., and Werb, Z. (2002) Inflammation and cancer (review). *Nature (London)* 420, 860–867
51. Bol, D. K., Rowley, R. B., Ho, C. P., Pilz, B., Dell, J., Swerdel, M., Kiguchi, K., Muga, S., Klein, R., and Fischer, S. M. (2002) Cyclooxygenase-2 overexpression in the skin of transgenic mice results in suppression of tumor development. *Cancer Res.* 62, 2516–2521
52. Weidner, N., Semple, J. P., Welch, W. R., and Folkman, J. (1991) Tumor angiogenesis and metastasis–correlation in invasive breast carcinoma. *N. Engl. J. Med.* 324, 1–8
53. Zhang, X., Morham, S. G., Langenbach, R., and Young, D. A. (1999) Malignant transformation and antineoplastic actions of nonsteroidal antiinflammatory drugs (NSAIDs) on cyclooxygenase-null embryo fibroblasts. *J. Exp. Med.* 190, 451–459

Received for publication May 13, 2004.
Accepted for publication October 8, 2004.

Sensitivity to gefitinib (Iressa, ZD1839) in non-small cell lung cancer cell lines correlates with dependence on the epidermal growth factor (EGF) receptor/extracellular signal-regulated kinase 1/2 and EGF receptor/Akt pathway for proliferation

Mayumi Ono,[1] Akira Hirata,[1] Takuro Kometani,[1] Miho Miyagawa,[1] Shu-ichi Ueda,[1] Hisafumi Kinoshita,[2] Teruhiko Fujii,[3] and Michihiko Kuwano[3]

[1]Department of Medical Biochemistry, Graduate School of Medical Sciences, Kyushu University, Fukuoka, Japan and [2]Department of Surgery and [3]Research Center for Innovative Cancer Therapy of the 21st Century COE Program for Medical Science, Kurume University, Fukuoka, Japan

Abstract

Gefitinib (Iressa, ZD1839), a quinazoline tyrosine kinase inhibitor that targets the epidermal growth factor receptor (EGFR), is approved for patients with advanced non-small cell lung cancer (NSCLC) in several countries including Japan. However, the mechanism of drug sensitivity to gefitinib is not fully understood. In this study, we examined the molecular basis of sensitivity to gefitinib using nine human lung cancer cell lines derived from NSCLC. PC9 was the most sensitive to gefitinib of the nine NSCLC cell lines when assayed either by colony formation or MTS assays. The various cell lines expressed different levels of EGFR, HER2, HER3, and HER4, but there was no correlation between levels of EGFR and/or HER2 expression and drug sensitivity. Phosphorylation of EGFR, protein kinase B/AKT (Akt), and extracellular signal-regulated kinase (ERK) 1/2 was inhibited by much lower concentration of gefitinib in PC9 cells than in the other eight cell lines under exponential growing conditions. About 80% of cell surface EGFR in PC-9 was internalized within 10 min, whereas only about 30–50% of the cell surface EGFR was internalized in more drug-resistant cell lines in 15–60 min. The present study is the first to demonstrate that sensitivity to growth inhibition by gefitinib in NSCLC cell lines under basal growth condition is associated with dependence on Akt and ERK1/2 activation in response to EGFR signaling for survival and proliferation and also that drug sensitivity may be related to the extent of EGF-induced down-regulation of cell surface EGFR. [Mol Cancer Ther. 2004;3(4):465–472]

Received 8/29/03; revised 1/24/04; accepted 1/28/04.

Grant support: Grant-in-aid for cancer research from Ministry of Education, Culture, Sports, Science and Technology, and Ministry of Health, Labor and Welfare, Japan.

The costs of publication of this article were defrayed in part by the payment of page charges. This article must therefore be hereby marked advertisement in accordance with 18 U.S.C. Section 1734 solely to indicate this fact.

Note: Iressa is a trademark of the AstraZeneca group of companies.

Requests for Reprints: Mayumi Ono, Department of Medical Biochemistry, Graduate School of Medical Sciences, Kyushu University, 3-1-1 Maidashi, Higashi-ku, Fukuoka 812-8582, Japan. Phone: 81-92-642-6098; Fax: 81-92-642-6203. E-mail: mayumi@biochem1.med.kyushu-u.ac.jp

Introduction

Epidermal growth factor receptor (EGFR) is a prototypical member of the EGFR family that includes HER2/neu (ErbB2), HER3 (ErbB3), and HER4 (ErbB4) (1–3). EGFR responds to a number of growth factors such as EGF/TGFα and amphiregulin. This family of receptors plays critical roles in the operation of signaling networks affecting proliferation, migration, survival, adhesion, and differentiation (3). EGFR and/or HER2 are highly expressed in many tumors of epithelial origin, including cancers of lung, breast, head and neck, and bladder (4), and patients whose tumors express high levels of EGFR and/or HER2 have a poor prognosis (5). EGFR family members exist as monomers spanning the plasma membrane, and the monomeric receptors dimerize and become functionally active after binding to the appropriate soluble extracellular ligand. Signal transduction is mediated by a large family of EGF receptors and their ligands (6). Homo- and/or heterodimerization of EGFR activates a number of intracellular signal transducing elements such as phospholipase Cγ, phosphatidylinositol-3′-kinase, protein kinase B/AKT (Akt), a small G-protein (Ras), the Ras GTPase-activating protein, extracellular signal-regulated kinase (ERK) 1/2, Src family kinases, and STATs (7). We have reported that the angiogenesis signal also operates through the EGF-EGFR pathway (8).

Agents that target tyrosine kinase receptors may contribute to the treatment of malignancies that have relatively high levels of EGFR expression (9, 10). The tyrosine kinase inhibitor gefitinib (Iressa, ZD1839) is a synthetic anilinoquinazoline that targets EGFR (11); it has good oral bioavailability, and antitumor activity in a broad range of mouse xenograft models (9) and tumor cell lines (12). Clinically meaningful antitumor activity was observed in two phase II trials of gefitinib monotherapy in previously treated patients with advanced non-small cell lung cancer, NSCLC (IDEAL 1 and 2), and gefitinib is now approved in several countries including Japan, Australia, and the United States for the treatment of

advanced NSCLC (13, 14). Concerning the basis of the differential sensitivity of human malignancies to the antitumor effect of gefitinib, animal experiments with xenografts of human breast cancer and other epithelial tumor cell lines have shown that tumors that overexpress HER2 are the most sensitive to gefitinib (15, 16). However, it could be argued that EGFR and/or HER2 levels (17, 18), or phosphorylation of EGFR, or other EGF/TGFα signaling mechanisms (19) control the sensitivity of cancer cells to gefitinib. Naruse *et al.* (20) have reported that a human leukemic cell line resistant to phorbol ester was 400-fold more sensitive to gefitinib than its parent, suggesting that gefitinib is most effective against cancer cells with non-P-glycoprotein-mediated multidrug resistance. In the present study, we investigated the basis of sensitivity to gefitinib in nine human cancer cell lines derived from NSCLC and two epidermoid cancers as controls. We tested whether the expression levels of EGFR family receptors and Cbl, EGFR phosphorylation, activation of EGFR downstream effectors such as Akt, or ERK1/2, and EGF-induced down-regulation were correlated with sensitivity to gefitinib.

Materials and Methods

Materials

Gefitinib was provided by AstraZeneca (Macclesfield, United Kingdom) (8). Recombinant human EGF was purchased from PeproTech (London, United Kingdom). Anti-EGFR antibody and anti-phospho-EGFR antibody were purchased from Upstate Biotechnology (Lake Placid, NY). Antibodies to ERK1/2, phospho-ERK1/2, Akt, and phospho-Akt were from Cell Signaling Technology (Beverly, MA). ^{125}I-protein A was purchased from Amersham Biosciences Corp. (Piscataway, NJ).

Cell Culture

Cell lines H522, H322, H358 (American Type Culture Collection, Manassas, VA), QG56 and PC9 (Kyushu Cancer Center, Fukuoka, Japan), and LK2 (Japanese Collection of Research Bioresources, Tokyo, Japan) were cultured in RPMI supplemented with 10% fetal bovine serum (FBS). A549 (Japanese Collection of Research Bioresources) was cultured in MEM supplemented with 10% FBS and NEAA. EBC-1 (Japanese Collection of Research Bioresources) was cultured in MEM supplemented with 10% FBS, and human epidermoid carcinoma KB3-1 cells were cultured in MEM supplemented with 10% newborn calf serum. LK2/EGFR-2 and LK2/EGFR-5 cells were established after stable transfection with PIRE/EGFRShyg1 expression plasmids using Lipofectin 2000 Reagent (Invitrogen, Corp., Carlsbad, CA). They were cultured in RPMI supplemented with 10% FBS and 350 μg/ml hygromycin. Cells were maintained under standard cell culture conditions at 37°C and 5% CO_2 in a humid environment.

Colony Formation Assay

Cell survival was determined by plating 3–9 × 10^2 cells in 35-mm dishes. After 24 h, various concentrations of gefitinib were added, followed by incubation for 7–10 days at 37°C. Gefitinib was solubilized in DMSO and controls for all experiments were carried out by adding equivalent volumes of DMSO. Colonies were counted after Giemsa staining, as described previously (21). IC_{50} values and SDs were obtained from the best fit of the data to a sigmoidal curve using GraphPad software.

Cell Viability Assay

CellTiter-Glo Luminescent Cell Viability Assay Kit (Promega Corp., Madison, WI) was used to evaluate cytotoxicity in LK2 and its stable transfectants. One hundred microliter aliquots of exponentially growing cell suspension (3–5 × 10^3 cells) were seeded into 96-well plates, and 24 h later, various concentrations of gefitinib were added. After incubation for 72 h at 37°C, 100 μl of CellTiter-Glo reagent were added and luminescence measured with a multilabel counter (Wallac, Tokyo, Japan). Each experiment was performed in three replicate wells for each drug concentration.

MTS Assay

A CellTiter 96^R AQ$_{ueous}$ One Solution Cell Proliferation Assay Kit (Promega) was used to evaluate cytotoxicity. One hundred microliter samples of an exponentially growing cell suspension (5–8 × 10^3 cells) were seeded into a 96-well microtiter plate, and various concentrations of gefitinib were added. After incubation for 72 h at 37°C, 20 μl of CellTiter 96^R AQ$_{ueous}$ One Solution were added to each well and the plates were incubated for a further 4 h at 37°C. Absorbance was measured at 490 nm with a 96-well plate reader. Each experiment was performed in three replicate wells for each drug concentration. The IC_{50} value is defined as the concentration needed for a 50% reduction in absorbance calculated from the survival curves.

Western Blot Analysis

To examine EGF-stimulated phosphorylation of proteins, confluent tumor cells were cultured in serum-free medium for 24 h. The cells were pretreated with gefitinib at concentrations up to 5 μM for 3 h before exposure to 20 ng/ml EGF for 15 min at 37°C. To examine phosphorylation under basal conditions, subconfluent tumor cells cultured in medium supplemented with 10% FBS were incubated with various concentrations of gefitinib for 3 h at 37°C. The cells were then rinsed with ice-cold PBS and lysed in Triton X-100 buffer. The cell lysates were subjected to SDS-PAGE and transferred to Immobilon membranes (Millipore, Bedford, MA). After transfer, the blots were incubated with blocking solution and probed with various antibodies followed by washing. Proteins were visualized with HRP-conjugated secondary antibodies followed by enhanced chemiluminescence (ECL, Amersham).

EGFR Down-Regulation

Confluent cells in 24-well dishes were incubated with or without 500 ng/ml of EGF for up to 1 h at 37°C in binding medium (0.1% bovine serum albumin in RPMI). Then the cells were washed twice with PBS to remove EGF and incubated for 1 h at 4°C with a 1:100 dilution of anti-EGFR monoclonal antibody recognizing the extracellular domain of human EGFR. After washing, the cells were incubated with 20,000 cpm/ml of ^{125}I-protein A (0.5 ng/ml) for 1 h at 4°C in binding medium. The cells were again washed and

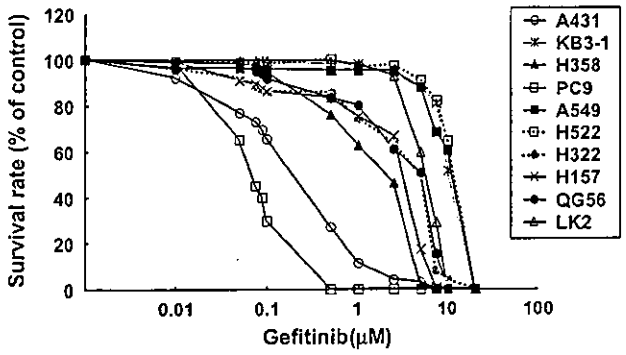

Figure 1. Dose-response curves of 10 human cancer cell lines, including 8 NSCLC lines and 2 epidermoid cancer lines, to gefitinib. Cell survival was determined by colony formation assay in the absence or presence of various doses of gefitinib. Number of colonies after incubation for 7 days with or without gefitinib were presented when normalized by colony numbers in the average of duplicate dishes. The IC_{50} for each cell line was presented from dose-response curves. Almost all cell lines except one line named EBC-1 were found to form colonies.

lysed with 1 N NaOH to determine the fraction of radioactivity (22). The linear regression coefficient of the dependence of this ratio on time represents the specific rate constant for down-regulation (K_e).

Results

Sensitivity to Gefitinib in NSCLC and Epidermoid Carcinoma Cell Lines

We first compared the effect of gefitinib on a panel of nine NSCLC cell lines, and two epidermoid carcinoma cell lines as controls, by both colony formation and MTS assay. Eight of the nine NSCLC cell lines and the two epidermoid cancer cell lines showed considerable resistance to gefitinib. Dose-response curves to gefitinib for 10 of the 11 human cancer cell lines assessed by the colony formation assay are presented in Fig. 1, and IC_{50} values for the 11 cell lines are given in Table 1. The seven NSCLC lines, A549, H522, H322, H358, H157, QG56, and LK2 showed 100- to 200-fold greater resistance to gefitinib than PC9 cells; the latter had an IC_{50} of 0.06 μM. The drug sensitivity of all 11 human cancer cell lines was also examined by MTS assay, and the IC_{50} values are also presented in Table 1. By the MTS assay, the IC_{50} of PC9 was 4 μM, and A549, H522, H322, H358, EBC-1, H157, QG56, and LK2 had 5- to 10-fold greater resistance to gefitinib (Table 1). In the colony formation assay, one of the epidermoid carcinoma cell lines, KB3-1, showed 25-fold higher resistance to gefitinib than the other cell line, A431, which had an IC_{50} of 0.4 μM (Fig. 1 and Table 1). When assayed by the MTS assay, the KB3-1 cells showed only a 2-fold higher resistance to gefitinib than the A431 cells (Table 1). Although the relative resistance of the other NSCLC and epidermoid cell lines compared with PC9 and A431 cells was much less when assayed by MTS than by colony formation, both assays concurred in indicating that the PC9 and A431 cells were more sensitive to gefitinib than the other cell lines examined in this study.

Expression of EGFR and Its Family of Receptor Proteins, HER2, HER3, and HER4

We examined expression of EGFR, HER2, HER3, and HER4 in all the cell lines used in this study by Western blot analysis. Expression of EGFR and its family members, HER2, HER3, and HER4, in the NSCLC cell lines varied considerably (Fig. 2). The level of expression of the receptors in each of the NSCLC and epidermoid cancer cell line is given in Fig. 2 relative to expression levels in the drug-sensitive lines PC9 and A431, respectively. One of the

Table 1. Cell lines employed in this study, sensitivities to gefitinib, and EGF-induced stimulation of EGFR, Akt, and ERK1/2

Cell Lines	Origin	IC_{50} (μM)[a]		Fold Stimulation by EGF[b]		
		Colony Formation	MTS	EGFR	Akt	ERK1/2
PC9	Human NSCLC (Adenocarcinoma)	0.06 (1.0)	4 (1.0)	1.6	4.0	2.9
A549	Human NSCLC (Adenocarcinoma)	13 (217)	21 (5.3)	3.5	11.1	15.6
H522	Human NSCLC (Adenocarcinoma)	13 (217)	20 (5.0)	2.4	1.9	4.5
H322	Human NSCLC (Adenocarcinoma)	6.8 (113)	27 (6.8)	6.6	2.8	1.7
H358	Human NSCLC (Adenocarcinoma)	2.0 (33)	12 (3.0)	3.2	2.1	8.8
EBC-1	Human NSCLC (Squamous cell carcinoma)	ND[c]	21 (5.3)	1.3	1.1	1.4
H157	Human NSCLC (Squamous cell carcinoma)	12 (200)	30 (7.5)	125	4.1	2.3
QG56	Human NSCLC (Squamous cell carcinoma)	7.8 (130)	42 (10.5)	1.5	3.8	12.7
LK2	Human NSCLC (Squamous cell carcinoma)	8.0 (133)	20 (5.0)	nd[d]	3.3	3.2
A431	Human epidermoid carcinoma	0.4 (1.0)	10 (1.0)	1.6	1.8	8.7
KB3-1	Human epidermoid carcinoma	10 (25)	15 (1.5)	31.3	4.2	6.9

[a]Drug sensitivity of nine human non-small lung cancer cell lines and two epidermoid cancer cell lines to gefitinib was assayed by both colony formation and MTS. IC_{50} value for each cell line is presented from two independent assays, and relative activity is presented in parentheses when normalized by IC_{50} for PC9 cells.
[b]The fold stimulation by EGF of EGFR, Akt, and ERK 1/2 is presented for each cell line when normalized by untreated control in the absence of EGF (see Fig. 4).
[c]ND, not determined because of poor colony-forming ability of the cell line.
[d]nd, not detected because of poor phosphorylation.

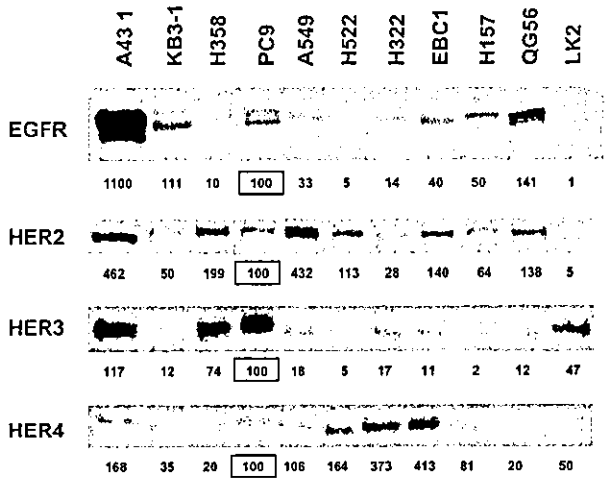

Figure 2. Protein expression of four EGFR family members, EGFR, HER2, HER3, and HER4, in nine NSCLC lines and two epidermoid carcinoma cell lines. Cellular protein levels of four EGFR family proteins were determined by Western blot analysis using specific antibodies. Each lane was analyzed with 100 μg protein of cell lysates from each cell line. Relative expression protein levels for NSCLC and epidermoid cancer cell line are presented when protein level of each EGFR family for PC9 and A431 is presented as 100%.

NSCLC cells, LK2 that expressed almost no detectable EGFR and HER2, was relatively resistant to gefitinib. On the other hand, QG56 cells that expressed more EGFR than PC9 cells were much less sensitive than the latter to gefitinib (Table 1). Expression of the four family members, EGFR, HER2, HER3, and HER4, varied among the NSCLC cell lines. Of two epidermoid cancer cell lines, gefitinib-resistant KB3-1 cells had only 10% of the EGFR level of A431 cells. In contrast, five of the NSCLC cell lines (H358, A549, H522, EBC1, QG56) had more HER2, while four NSCLC cell lines had lower levels of HER3 than PC9. KB3-1 cells had 10–20% of the EGFR, HER2, HER3, and HER4 of A431 cells (Fig. 2). Thus, expression of the four EGFR family members is not correlated with the cytotoxicity of gefitinib. We next examined if increasing the expression of EGFR in LK2 cells, which expressed very low levels, if any, of EGFR (see Fig. 2) would render them sensitive to gefitinib. Two EGFR transfectants (LK2/EGFR-2 and LK2/EGFR-5) were isolated by introducing cDNA of human EGFR into the LK2 cells. These EGFR transfectants had much higher EGFR levels than their parent, or mock transformed LK2 cells (Fig. 3A). However, their sensitivity to gefitinib was similar to that of the parent strain when assayed by the cell viability assay (Fig. 3B).

Effect of Gefitinib on Phosphorylation of EGFR, Akt, and ERK1/2

EGF/TGFα causes phosphorylation of EGFR by its tyrosine kinase activity, and leads to activation of a number of downstream cytoplasmic signaling molecules (6). We first examined the effect of gefitinib on phosphorylation of EGFR, Akt, and ERK1/2 in response to EGF (EGF-induced phosphorylation) in the cell lines used in this study.

Figure 4 shows the inhibitory effect of gefitinib on EGF-induced autophosphorylation of EGFR, and phophorylation of Akt and ERK1/2 in three of the NSCLC cell lines. EGF stimulated EGFR autophosphorylation and activation of Akt and ERK1/2 in PC9 (A), A549 (B), and QG56 (C) cells, and activation was blocked to different extents by gefitinib. Table 2 presents IC_{50} (μM) values for EGF-induced autophosphorylation of EGFR, and for phosphorylation of Akt and ERK1/2. IC_{50} gefitinib doses for EGF-induced autophosphorylation of EGFR were similar in all the NSCLC cell lines including PC9 although the drug-resistant lines EBC-1 and H157 had 2.7- and 0.2-fold higher IC_{50} (μM) values. EGF-induced Akt phosphorylation in four of the NSCLC cell lines was 10-fold or more resistant to gefitinib than in PC9 cells while the other cell lines showed similar IC_{50} values to PC9. ERK1/2 phosphorylation was highly

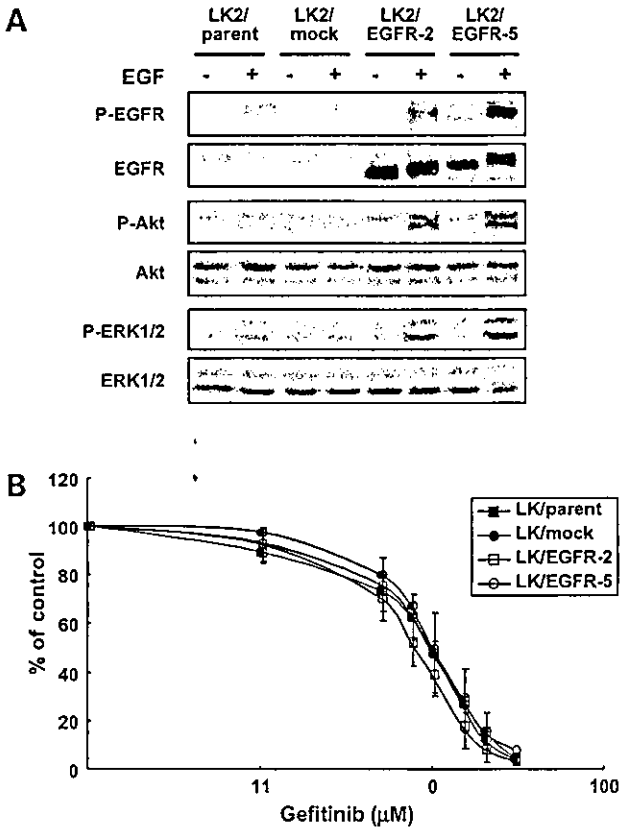

Figure 3. Protein expression of EGFR in LK2 and its two EGFR transfectants (LK2/EGFR2 does not alter sensitivity to gefitinib in LK2 cells). **A**, comparison of EGFR, Akt, and ERK1/2 protein expression levels and phosphorylation of EGFR, Akt, and ERK1/2 with or without EGF in a subclone of LK2 cells transfected with EGFR or mock vector. Serum-starved cells were treated with 20 ng/ml EGF for 10 min. Protein extracts were resolved by 7.5% SDS-PAGE and probed with either antibody. Immunoreactive proteins were visualized by enhanced chemiluminescence. **B**, dose-response curves of a subclone of LK2 cells transfected with EGFR or mock vector to gefitinib. Sensitivity to gefitinib was determined by cell viability assay in the absence or presence of various doses of gefitinib. The number of viable cells was calculated at 72 h and graphed as percentage of untreated cells. *Points*, average of triplicate dishes; *bars*, SD.

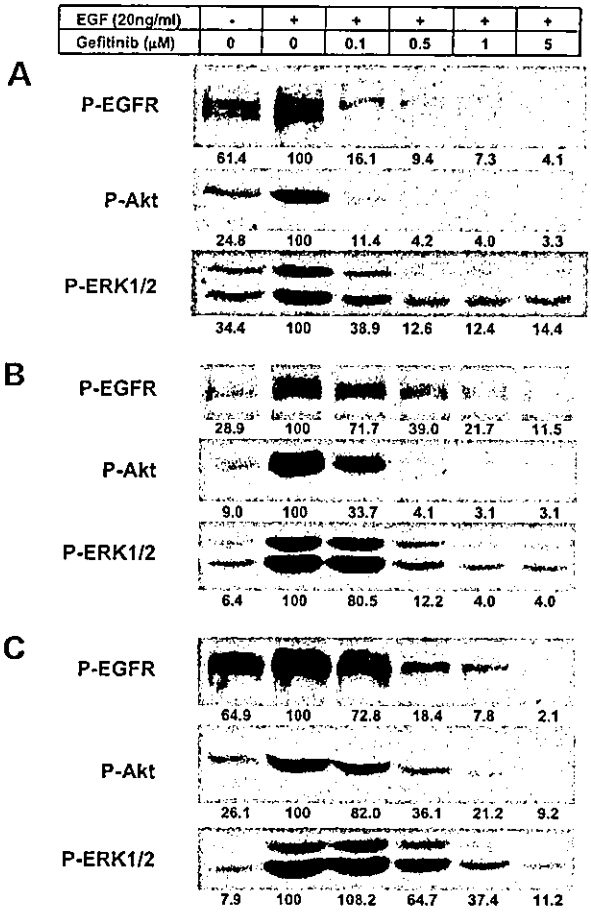

Figure 4. Dose-dependent inhibition of EGF-induced EGFR autophosphorylation, Akt and ER1/2 phosphorylation in three human cancer cells. Serum-starved cancer cells were treated for 3 h with the indicated concentrations of gefitinib, followed by the addition of EGF (20 ng/ml) for 15 min. Protein extracts were resolved by 7.5% SDS-PAGE and probed with either antibody. Immunoreactive proteins were visualized by enhanced chemiluminescence. **A**, PC9 cells; **B**, A549 cells; and **C**, QG56 cells.

resistant to gefitinib in most of the NSCLC cell lines, while the remaining three were only weakly resistant (1.1- to 3.1-fold). The two epidermoid carcinoma cell lines, A431 and KB3-1, showed similar IC_{50} values for gefitinib with respect to EGFR, Akt, and ERK1/2 phosphorylation (Table 2).

Figure 5 presents the effects of gefitinib on phosphorylation of EGFR, Akt, and ERK1/2 in three cell lines under basal growth condition in the presence of 10% serum. EGFR autophosphorylation and activation of Akt and ERK1/2 in PC9 (A), A549 (B), and QG56 (C) cells were inhibited to different extents. In PC9 cells, EGFR autophosphorylation as well as Akt and ERK1/2 activation were almost completely blocked by 0.1 μM gefitinib (Fig. 5A). By contrast, in the other two cell lines, A549 and QG56, there was only slight if any inhibition of the activation of Akt and ERK1/2 despite the fact that EGFR phosphorylation was completely inhibited at 0.5–5 μM (Fig. 5, B and C). Under basal growth condition, all three processes, EGFR autophosphorylation and activation of Akt and ERK1/2 were the most susceptible to inhibition by gefitinib in PC9 cells. The IC_{50} for EGFR autophosphorylation was only 0.07 μM in PC9 while the IC_{50} values in the other cell lines were about 4-fold or more higher. KB3-1 cells also showed a 3-fold higher IC_{50} for EGFR autophosphorylation than the A431 cells. Gefitinib inhibited Akt activation under basal growth condition with an IC_{50} of 0.08 μM in PC9, whereas the IC_{50} values for QG56 and the other seven cell lines were 4- to 125-fold higher. The dose of gefitinib to inhibit ERK1/2 activation in PC9 cells under basal growth condition was almost 200-fold lower than that required to inhibit the other seven NSCLC cell lines (Table 2). The IC_{50} value for ERK1/2 activation in H358 cells was about 3-fold higher than in PC9 cells, while the IC_{50} values for both Akt and ERK1/2 phosphorylation in KB3-1 were much higher than in the drug-sensitive A431 cells (Table 2).

Table 2. Inhibition by gefitinib of EGF-induced and basal phosphorylation of EGFR, Akt, and ERK1/2 in nine NSCLC and two epidermoid carcinoma cells

Cell Lines	EGF-Induced (IC_{50}, μM)[a]			Basal Condition (IC_{50}, μM)		
	P-EGFR	P-Akt	P-ERK1/2	P-EGFR	P-Akt	P-ERK1/2
PC9	0.30 (1.0)	0.05 (1.0)	0.07 (1.0)	0.07 (1.0)	0.08 (1.0)	0.03 (1.0)
A549	0.22 (0.7)	0.06 (1.2)	0.22 (3.1)	0.25 (3.6)	5< (63<)	5< (167<)
H522	0.30 (1.0)	0.50 (10)	0.40 (5.7)	0.50 (7.1)	5 (63)	5< (167<)
H322	0.43 (1.4)	0.13 (2.0)	5< (71<)	0.35 (5.0)	5< (63<)	5< (167<)
H358	0.40 (1.3)	0.13 (2.0)	0.75 (11)	5 (71)	5< (63<)	0.1 (3.3)
EBC-1	0.80 (2.7)	5< (100<)	5< (71<)	5 (71)	10< (125<)	10< (333<)
H157	0.06 (0.2)	0.07 (1.4)	0.13 (1.9)	0.7 (10)	5 (63)	5< (167<)
QG56	0.20 (0.7)	0.90 (18)	2.20 (31)	0.3 (4.3)	0.35 (4.4)	5< (167<)
LK2	nd[b]	0.50 (10)	0.08 (1.1)	nd	10< (125<)	10< (333<)
A431	0.04 (1.0)	0.10 (1.0)	0.04 (1.0)	0.05 (1.0)	0.5 (1.0)	0.1 (1.0)
KB3-1	0.04 (1.0)	0.12 (1.2)	0.05 (1.3)	0.13 (2.6)	5 (10)	5< (50<)

[a] IC_{50} values were obtained from 50% inhibitory doses of gefitinib on phosphorylation of EGFR, Akt, and ERK1/2 under EGF-stimulated or basal (10% serum) culture condition as presented in Fig. 2. The relative activity for IC_{50} of each cell line is presented in parentheses when normalized by the IC_{50} value in PC9 and A431, respectively.
[b] nd, not detected because of poor phosphorylation.

EGF-Induced EGFR Down-Regulation and Expression of Cbl Protein

Cell surface EGFR is internalized during EGF/TGFα-driven receptor recycling in exponentially growing cells. We compared the rates of EGF-induced internalization of EGFR in the cell lines expressing relatively high amounts of EGFR (Fig. 6). After exposure to EGF, EGFR was rapidly down-regulated from the cell surface, and we found that 80% and 60% of the cell surface EGFR was internalized within 15 min in PC9 and A431 cells, respectively. In contrast, there was only 30–50% loss of cell surface EGFR 15–40 min after EGF stimulation in EBC-1, A549, and QG56 cells. Sixty percent to 80% of the EGFR molecules thus appeared to be rapidly internalized from the cell surface in gefitinib-sensitive cells, whereas much fewer EGFR molecules were internalized in the resistant cells and internalization was slower.

Cbl is a key protein limiting the initial step of EGFR endocytosis (6), and the EGFR signaling complex is degraded in a coordinate manner with Cbl after interacting with EGF (23). We examined expression of Cbl protein in the nine NSCLC cell lines and two epidermoid carcinoma cell lines (Fig. 7). Almost all the cell lines differed in their expression of Cbl with EBC-1 and QG56 cells expressing considerably less Cbl than the other cell lines. The relative expression levels of Cbl protein in both the NSCLC and epidermoid cancer cell lines are presented in Fig. 7. Cbl expression appears not to be correlated with either the rate of EGF-induced down-regulation (see Fig. 6) or sensitivity to gefitinib (Table 1).

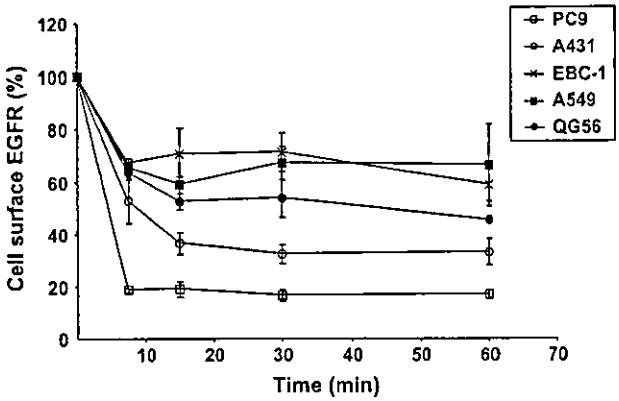

Figure 6. Time kinetics for EGF-induced down-regulation of EGFR. All cell lines (*PC9, EBC-1, A549, QG56, A431*) were further incubated with 500 ng/ml EGF at 37°C for the indicated periods. Then cells were incubated for 1 h at 4°C with a monoclonal antibody against human EGF receptor which specifically recognizes extracellular domain of EGFR and for another 1 h with ^{125}I-protein A. Relative amount of ^{125}I-protein A bound to the EGFR antibody is plotted and cell surface EGFR was determined by ^{125}I-protein A (see Materials and Methods; Ref. 22). *Points,* average of triplicate dishes; *bars,* SD.

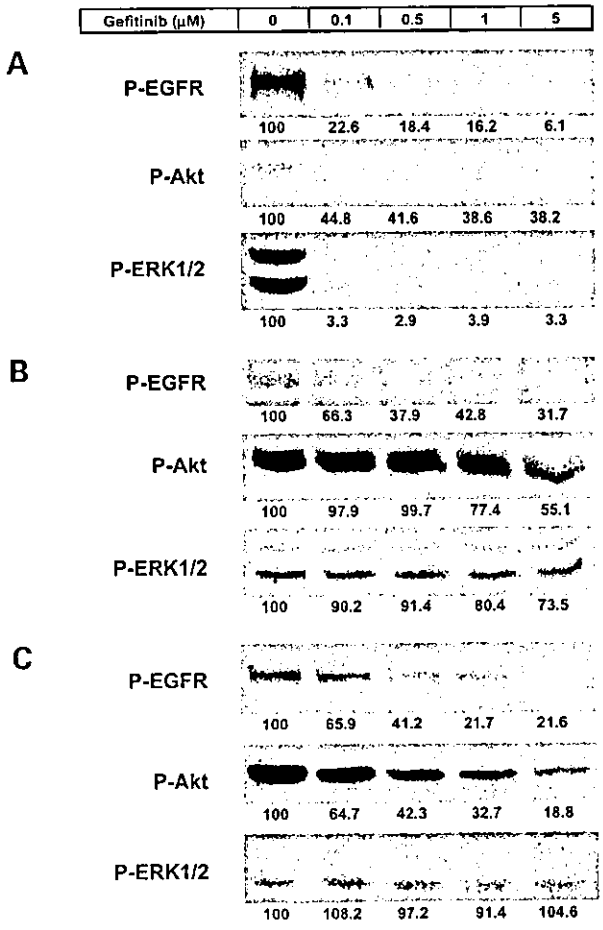

Figure 5. Dose-dependent inhibition by gefitinib of EGFR, Akt and ERK1/2 phosphorylation under basal growth conditions in three human cancer cell lines. Exponentially growing cells in 10% serum medium were pretreated for 3 h with the indicated concentrations of gefitinib. Protein extracts were resolved by 7.5% SDS-PAGE and probed with either antibody. EGFR, Akt, and ERK1/2 activity was determined using each corresponding anti-phospho antibody. Immunoreactive proteins were visualized by enhanced chemiluminescence. A, PC9 cells; B, A549 cells; and C, QG56 cells.

Discussion

Of the nine NSCLC cell lines, PC9, derived from an adenocarcinoma, was the most sensitive to the EGFR-targeting agent, gefitinib, and of the two epidermoid cancer cell lines, A431 was more sensitive to gefitinib than KB3-1. The sensitivity of PC9 was similar to that of A431. All these cell lines except LK2 expressed some, although variable, levels of EGFR, HER2, HER3, and HER4. EGFR expression in PC9 was similar to that of some of resistant NSCLC cell

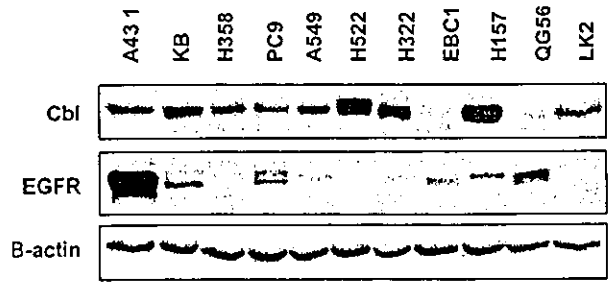

Figure 7. Expression of Cbl and EGFR protein in nine NSCLC cell lines and two epidermoid carcinoma cell lines. Protein levels of Cbl, EGFR, and β-actin determined by Western blot analysis using 100 μg protein of cell lysate of each cell line from NSCLC and EC lines are presented when PC9 (NSCLC) and A431 (EC) are respectively normalized as 100%.

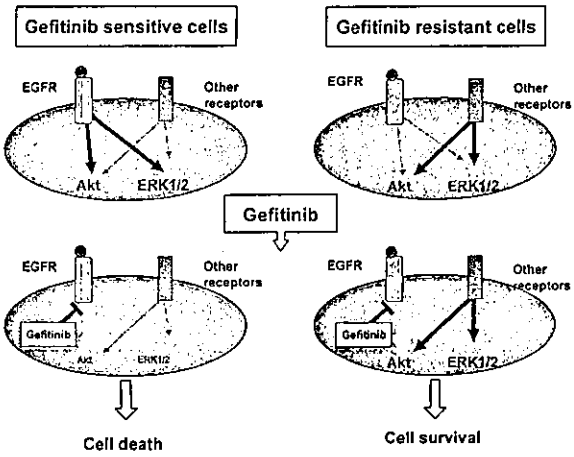

Figure 8. A model of how drug sensitivity to gefitinib is controlled in NSCLC and EC. From our present study, in gefitinib-sensitive cell lines (PC9 and A431), only EGFR-driven signaling following activation of both Akt and ERK1/2 was dominant for survival. On the other hand, in gefitinib-resistant cells, EGFR is not a survival factor and other factor or receptor-driven cell survival following activation of downstream signaling effectors was dominant. Therefore, cells, the survival and apoptosis of which are totally dependent on EGFR signaling, are highly susceptible to gefitinib.

lines. We also observed no apparent difference in sensitivity to gefitinib between LK2 and two EGFR derivatives (LK2/EGFR-2 and LK2/EGFR-5), suggesting that it is unlikely that the level of EGFR expression is directly associated with sensitivity to gefitinib. A related study by Moasser *et al.* (15) reported that tumors overexpressing HER2 were highly sensitive to gefitinib. However, our data show that HER2 expression was much higher in five of the drug-resistant NSCLC lines than in PC9 (Fig. 2). The expression of two other EGFR family members, HER3 and HER4, also varied among the nine NSCLC lines, suggesting again that it is also unlikely that cellular HER3 and HER4 levels are related to sensitivity to gefitinib. In the two epidermoid cancer lines, expression of the four EGFR family members was much higher in the gefitinib-sensitive A431 cells than in the KB3-1 cells. However, this correlation is not convincing because we only compared two cell lines.

Stimulation with EGF/TGFα and other ligands activates Akt, ERK1/2, and other molecules, and such EGFR signaling controls cell migration, adhesion, apoptosis, cell cycle progression, growth, and angiogenesis (3). In our present study, we examined the effect of gefitinib on EGFR autophosphorylation and the downstream signaling by ERK1/2 and Akt under both EGF-induced and basal growth condition (Table 2). When the cells were stimulated with EGF, exposure to gefitinib blocked EGFR autophosphorylation at similar concentrations in all NSCLC cell lines including PC9. Inhibition of EGF-induced phosphorylation of ERK1/2 required higher doses of gefitinib in all the other NSCLC lines than in PC9 (Table 2). Treatment with gefitinib also inhibited EGF-induced Akt phosphorylation at similar doses in five of eight NSCLC cell lines including PC9 cells. Therefore, EGF-induced EGFR autophosphorylation and Akt activation do not appear to be related to levels of sensitivity to gefitinib.

Under basal growth conditions in the presence of 10% serum, inhibition of EGFR autophosphorylation in seven of the NSCLC cell lines required 4-fold (or higher) levels of gefitinib than PC9 (Table 2). To our surprise, activation of both Akt and ERK1/2 in almost all the NSCLC lines was found to be much less susceptible to the inhibitory effect of gefitinib under basal growth condition than in the drug-sensitive PC9 cells (Table 2). The activation of EGFR, Akt, and ERK1/2 in A431 cells was also highly sensitive to inhibition in comparison with KB3-1. Taken together, these findings indicate that under basal growth condition, high sensitivity to gefitinib in NSCLC and epidermoid cancer lines is closely correlated with dependence on Akt and ERK1/2 activation in response to EGFR signaling for survival and proliferation (see Fig. 8). Consistent with this notion, Barnes *et al.* (24) have reported that gefitinib inhibited EGFR and mitogen-activated protein kinase (MAPK) activation efficiently in exponentially growing cutaneous carcinoma cells.

We also observed an apparent difference in EGF-induced down-regulation of cell surface EGFR between drug-sensitive PC9 or A431 cells and drug-resistant EBC-1, A549, QG56, and KB3-1 cells (see Fig. 6). Almost all cell surface EGFR molecules were rapidly internalized in PC9 or A431 cells when only 30–50% of the cell surface EGFR molecules were slowly internalized in gefitinib-resistant cell lines. EGFR molecules in the sensitive cell lines seem to be highly susceptible to EGF stimulation with the result that they transduce the signals more effectively than the drug-resistant cells. We also examined expression of Cbl protein (Fig. 7). Cbl is a key protein affecting receptor internalization in general. However, there was no correlation between level of Cbl protein and EGF-induced down-regulation of EGFR.

In conclusion, one NSCLC cell line, PC9, of the nine strains examined was especially sensitive to the effect of gefitinib. This sensitivity appears to follow from the fact that this cell line is much more dependent than the others on the EGF receptor/ERK1/2 and Akt pathway for its survival and proliferation (see Fig. 8). The sensitivity of the EGFR pathway could be useful for predicting the likely effectiveness of gefitinib in NSCLC patients. Further analysis of other signaling processes in addition to EGFR phosphorylation are called for using clinical specimens.

References

1. Mendlsohn J, Baserga J. The EGF receptor family as targets for cancer therapy. Oncogene, 2000;19:6550–65.

2. da Bono JS, Rowinsky EK. The ErbB receptor family: a therapeutic target for cancer. Trends Mol Med, 2002;8:19–26.

3. Woodburn JR. The epidermal growth factor receptor and its inhibition in cancer therapy. Pharmacol Ther, 1999;82:241–50.

4. Arteaga CL. Epidermal growth factor receptor dependence in human tumors: more than just expression? Oncologist, 2002;7:31–9.

5. Brabender J, Danenberg KD, Metzger R, et al. Epidermal growth factor receptor and HER2-neu mRNA expression in non-small cell lung cancer is correlated with survival. Clin Cancer Res, 2001;7:1850–5.

6. Yarden Y. The EGFR family and its ligands in human cancer signaling mechanisms and therapeutic opportunities. Eur J Cancer, 2001;37: 3–8.

7. Raymond E, Faivre S, Armand JP. Epidermal growth factor receptor tyrosine kinase as a target for anticancer therapy. Drugs, 2000;60:15–23; discussion 41–2.

8. Hirata A, Ogawa S, Kometani T, et al. ZD1839 (Iressa) induces antiangiogenic effects through inhibition of epidermal growth factor receptor tyrosine kinase. Cancer Res, 2002;62:2554–60.

9. Sirotnak FM, Zakowski MF, Miller VA, Scher HI, Kris MG. Efficacy of cytotoxic agents against human tumor xenografts is markedly enhanced by coadministration of ZD1839 (Iressa), a inhibitor of EGFR tyrosine kinase. Clin Cancer Res, 2000;6:4885–92.

10. Slichenmyer WJ, Fry DW. Anticancer therapy targeting the erbB family of receptor tyrosine kinases. Semin Oncol, 2001;28:67–79.

11. Baselga J, Averbuch SD. ZD1839 (Iressa) as an anticancer agent. Drugs, 2000;60:33–40; discussion 41–2.

12. Ciardiello FI, Caputo R, Bianco R, et al. Antitumor effect and potentiation of cytotoxic drug activity in human cancer cells by ZD1839 (Iressa), an epidermal growth factor receptor-selective tyrosine kinase inhibitor. Clin Cancer Res, 2000;6:2053–63.

13. Fukuoka M, Yano S, Giaccone G, et al. Multi-institutional randomized phase II trial of gefitinib for previously treated patients with advanced non-small-cell lung cancer. J Clin Oncol, 2003;21:2237–46.

14. Kris MG, Natale RB, Herbest RS, et al. A phase II trial of ZD1839 ('Iressa') in advanced non-small cell lung cancer (NSCLC) patients who had failed platinum- and docetaxel-based regimens (IDEAL 2). Proc Am Soc Clin Oncol, 2002;21:292a #1166.

15. Moasser MM, Basso A, Averbuch SD, Rosen N. The tyrosine kinase inhibitor ZD1839 ('Iressa') inhibits HER2-driven signaling and suppresses the growth of HER2-overexpressing tumor cells. Cancer Res, 2001;61:7184–8.

16. Moulder SL, Yakes FM, Muthuswamy SK, Bianco R, Simpson JF, Arteaga CL. Epidermal growth factor receptor (HER1) tyrosine kinase inhibitor ZD1839 (Iressa) inhibits HER2/neu (erbB2)-overexpressing breast cancer cells *in vitro* and *in vivo*. Cancer Res, 2001;61:8887–95.

17. Anderson NG, Ahmad T, Chan K, Dobson R, Bundred NJ. ZD1839 (Iressa), a novel epidermal growth factor receptor (EGFR) tyrosine kinase inhibitor, potently inhibits the growth of EGFR-positive cancer cell lines with or without erbB2 overexpression. Int J Cancer, 2001;94:774–82.

18. Bishop PC, Myers T, Robey R, et al. Differential sensitivity of cancer cells to inhibitors of the epidermal growth factor receptor family. Oncogene, 2002;21:119–27.

19. Magne N, Fischel JL, Dubreuil A, et al. Influence of epidermal growth factor receptor (EGFR), p53 and intrinsic MAP kinase pathway status of tumor cells on the antiproliferative effect of ZD1839 (Iressa). Br J Cancer, 2002;86:1518–23.

20. Naruse I, Ohmori T, Ao Y, et al. Antitumor activity of the selective epidermal growth factor receptor-tyrosine kinase inhibitor (EGFR-TKI) Iressa (ZD1839) in an EGFR-expressing multidrug-resistant cell line *in vitro* and *in vivo*. Int J Cancer, 2002;98:310–5.

21. Koike K, Kawabe T, Tanaka T, et al. A canalicular multispecific organic anion transporter (cMOAT) antisense cDNA enhances drug sensitivity in human hepatic cancer cells. Cancer Res, 1997;57:5475–9.

22. Ono M, Nakayama Y, Gopas JG, Kung J-H, Kuwano M. Polyoma middle T antigen or v-src desensitizes human epidermal growth factor receptor function and interference by a monensin-resistant mutation in mouse Balb/3T3 cells. Exp Cell Res, 1992;203:456–65.

23. Ettenberg SA, Magnifico A, Cuello M, et al. Cbl-b-dependent coordinated degradation of the epidermal growth factor receptor signaling complex. J Biol Chem, 2001;276:27677–84.

24. Barnes CJ, Bagheri-Yarmand R, Mandal M, et al. Suppression of epidermal growth factor receptor, mitogen-activated protein kinase, and Pak1 pathways and invasiveness of human cutaneous squamous cancer cells by the tyrosine kinase inhibitor ZD1839 (Iressa). Mol Cancer Ther, 2003;2:345–51.

Targeted disruption of one allele of the *Y-box binding protein-1* (*YB-1*) gene in mouse embryonic stem cells and increased sensitivity to cisplatin and mitomycin C

Kotaro Shibahara,[1,2] Takeshi Uchiumi,[1,7] Takao Fukuda,[1] Shinobu Kura,[3] Yohei Tominaga,[4] Yoshihiko Maehara,[2] Kimitoshi Kohno,[5] Yusaku Nakabeppu,[4] Teruhisa Tsuzuki[3] and Michihiko Kuwano[6]

[1]Departments of Medical Biochemistry, [2]Surgery and Science, [3]Medical Biophysics & Radiation Biology, [4]Faculty of Medical Sciences, Division of Neurofunctional Genomics, Medical, Institute of Bioregulation, Kyushu University, 3-1-1 Maidashi, Fukuoka 812-8582, [5]Department of Molecular Biology, University of Occupational and Environmental Health, Yahatanishi-ku, Kitakyushu 807-8555; and [6]Research Center for Innovative Cancer Therapy, 21st Century COE Program for Medical Science, Kurume University, 67 Asahimachi, Kurume, Fukuoka 830-0011

(Received January 7, 2004/Accepted February 4, 2004)

The eukaryotic Y-box binding protein-1 (YB-1) functions in various biological processes, including transcriptional and translational control, DNA repair, drug resistance, and cell proliferation. To elucidate the physiological role of the YB-1 protein, we disrupted one allele of mouse *YB-1* in embryonic stem (ES) cells. Northern blot analysis revealed that *YB-1*$^{+/-}$ ES cells with one intact allele contain approximately one-half the amount of mRNA detected in wild-type (*YB-1*$^{+/+}$) cells. We further found that the protein level of *YB-1*$^{+/-}$ cells was reduced to approximately 50–60% compared with that of *YB-1*$^{+/+}$ cells. However, no apparent growth difference was found between *YB-1*$^{+/-}$ and *YB-1*$^{+/+}$ cells. *YB-1*$^{+/-}$ cells showed increased sensitivity to cisplatin and mitomycin C, but not to etoposide, X-ray or UV irradiation, as compared to *YB-1*$^{+/+}$ cells. YB-1 may have the capacity to exert a protective role against cytotoxic effects of DNA damaging agents, and may be involved in certain aspects of drug resistance. (Cancer Sci 2004; 95: 348–353)

The Y-box protein family, which is widely distributed from bacteria to mammals, contains a cold-shock domain which is highly conserved from prokaryotic cold-shock proteins.[1] The human Y-box binding protein, YB-1, which is located on chromosome 1p34, was initially identified as a transcription factor which associates with the Y-box sequence appearing in the major histocompatibility complex class II genes.[2–4]

It has been hypothesized that YB-1 might play a role in promoting cell proliferation through the transcriptional regulation of various relevant genes, including proliferating cell nuclear antigen, epidermal growth factor receptor, DNA topoisomerase IIα, thymidine kinase, and DNA polymerase α.[5,6] In our laboratory, we have shown that YB-1 is involved in transcriptional activation of the human multidrug resistance 1 gene.[7–9] and also the DNA topoisomerase IIα gene[10] in response to various environmental stimuli. YB-1 appears to play a critical role in cell proliferation, DNA replication, and drug resistance. The biological roles of YB-1 include modification of chromatin, translational masking of mRNA, participation in the redox signaling pathway, RNA chaperoning, and stress response regulation.[11] It has also been demonstrated that eukaryotic Y-box proteins regulate gene expression at the translational level by recognizing RNA.[12,13] The murine YB-1 protein (MSY1) is specifically expressed in testis rather than other tissues, and regulates the translation of germ cell RNA.[14] The Y-box binding proteins thus appear to play critical roles in both mRNA turnover and translational control.

YB-1 also appears to protect mammalian cells from the cytotoxic effects induced by DNA damage. We have previously reported that human cancer cell lines overexpressing YB-1 showed resistance to cisplatin, while the reduction of YB-1 itself leads to increased drug sensitivity to cisplatin, other DNA-interacting drugs, and UV irradiation.[15] We also demonstrated that YB-1 protein is localized mainly in the cytoplasm, but translocates to the nucleus when cells are irradiated with UV or treated with anticancer drugs.[16] YB-1 specifically binds to cisplatin-modified DNA, apurinic DNA and also 8-oxo-guanine-containing RNA.[17–19] We have further demonstrated that YB-1 binds directly to repair-associated proteins such as proliferating cell nuclear antigen and p53 protein.[18,20] YB-1 may thus be involved in the process of DNA repair and/or DNA damage response. In clinical studies on YB-1, the cellular level of YB-1 was found to be closely associated with tumor growth and prognosis in ovarian cancers, lung cancers, and breast cancers.[21–23]

To gain more insight into how YB-1 proteins exert their multiple functions, we carried out a targeted disruption of the *mouse YB-1* gene (*MSY1*) in mouse embryonic stem (ES) cells. We have established ES cell lines with a heterozygously targeted disruption of the *YB-1* gene (*YB-1*$^{+/-}$), which we found to result in hypersensitivity to cytotoxic agents, such as cisplatin and mitomycin C.

Materials and Methods

Cell growth characteristics. CCE ES cells and YB-1 knockout cells were maintained on a feeder cell layer in DMEM supplemented with 20% heat-inactivated fetal bovine serum and 100 units/ml of recombinant leukemia inhibitory factor at 37°C in an atmosphere of 10% CO_2 in air.

Construction of the targeting vector. The mouse *YB-1* gene was isolated from a 129/Sv genomic library by the standard plaque hybridization method, using mouse *YB-1* cDNA as a probe. The targeting vector contained approximately 8.4 kb of genomic sequence interrupted by a *pol*II-*neo*-poly(A) cassette. Insertion of the neomycin (*neo*) cassette resulted in deletion of a 1.8-kb *Sal*I/*Bgl*II fragment of the *YB-1* gene, containing 43 nucleotides of exon 5 and 84 nucleotides of exon 6, as well as 240 nucleotides of intron 5 and 1.4 kb of intron 6. A pair of herpes simplex virus thymidine kinase (TK) cassettes (TK1 and TK2, both under control of the MC1 promoter) were placed flanking

[7]To whom correspondence should be addressed.
E-mail: uchiumi@biochem1.med.kyushu-u.ac.jp

Abbreviations: YB-1, Y-box binding protein-1; ES, embryonic stem; MTS, [3-(4,5-dimethylthiazol-2-yl)-5-(3-carboxymethoxyphenyl)-2-(4-sulfophenyl)-2*H*-tetrazolium, inner salt; PES, phenazine ethosulfate.

the *YB-1* genomic sequence in the targeting vector to allow for positive and negative selection of DNA when introduced into ES cells.[24] The targeting construct was linearized at a unique *Not*I site located on the plasmid vector.

Isolation of heterozygous mutant embryonic stem cell lines. The ES cell line CCE was cultured on a feeder cell layer and electroporated, using 5×10^7 cells and 50 μg of the linearized targeting vector DNA, as described.[25] The transfected cells were subjected to positive and negative selection, using G418 (250 μg/ml; Geneticin, GIBCO/BRL) and ganciclovir (GANC) (5 m*M*; a gift of Nihon Syntex) as selective agents. Colonies doubly resistant to G418 and GANC were grown on 24-well plates to expand them for Southern blot analysis. DNA was isolated from each cell line and analyzed by Southern blot hybridization.

Southern blot analysis. Genomic DNA (8 μg) was digested with *Eco*RV and *Bgl*II, then run on a 0.7% agarose gel and transferred to a nylon membrane filter (Hybond N1; Amersham). The filter was hybridized with a 0.3-kb *Eco*RV/*Eco*RI fragment (5′ internal probe A) and a 0.3-kb *Xho*I/*Hin*dIII fragment (3′ flanking probe B), labeled with [α-^{32}P]dCTP. The membrane was washed, applied to an imaging plate, and analyzed using a Bio-image analyzer BAS 2000 (Fuji Photo Film Co., Kanagawa).

RNA isolation and northern blot analysis. Cells in the exponential growth phase were transferred to a medium without feeder layer cells and further cultured on a gelatin-coated dish for 4 days to avoid contamination with *YB-1* mRNA derived from feeder cells. Total RNA was isolated using an RNeasy spin column (Qiagen, Hilden, Germany). RNA samples (10 μg/lane) were separated on a 1% formaldehyde-agarose gel and were transferred to a membrane. The membranes were hybridized with ^{32}P-labeled mouse YB-1 1.2-kb cDNA as a probe.[15] Radioactivity was visualized by autoradiography and was analyzed using a Fujix Bas 2000 bioimaging analyzer (Fuji Photo Film Co., Tokyo).

Immunoblotting of the YB-1 protein. The cells were lysed in TNE buffer (50 m*M* Tris-HCl (pH 7.5), 150 m*M* NaCl, 1 m*M* EDTA, 0.5% NP-40, 1 m*M* PMSF, 10 μg/ml leupeptin, 10 μg/ml aprotinin), and boiled in western sample buffer for 10.0% SDS-PAGE and western blot analysis. An antibody to YB-1 was generated as described previously.[15] PCNA-specific antibody (PC10; Santa Cruz) and p21 (sc-817; Santa Cruz) were used for western blotting.

Proliferation rates. To determine the proliferation rates of ES cells, 5×10^5 cells were plated in triplicate in 6-well plates and the cell numbers were determined at the indicated time points using a CASYR cell counter.

Clonogenic survival assay. ES cells were plated on gelatin-coated 6-well plates at a density of approximately 500 cells/well. Twenty-four hours after plating, ES cells were treated with various chemical agents, X-rays or UV irradiation. Plates were incubated for 7 days and the surviving ES cell colonies in each well were counted after staining with Giemsa. The plating efficiency was ~60–80%. The relative sensitivity of each clone of *YB-1*$^{+/-}$ ES cells was determined by dividing the IC_{90} value for each cell line by that of wild-type (*YB-1*$^{+/+}$) ES cells.

MTS survival assay. CellTiter 96 Aqueous One Solution cell proliferation Assay (Promega) was used to evaluate drug sensitivities. The 96-well plates were inoculated with 4000 cells/well in a volume of 100 μl of ES medium. Twenty-four hours later, drugs were added at various concentrations. Seventy-two hours later, 20 μl of MTS/PES was added, and incubation was continued for 2 h at 37°C. In the presence of the electron-coupling reagent PES, MTS is reduced by dehydrogenase enzymes found in metabolically active cells into a formazan product that is readily soluble in tissue culture medium. The quantity of formazan product was measured in terms of the absorbance at 490 nm. At least five different drug concentrations were used to determine the IC_{50} values, and each drug concentration was replicated in 4 wells for each individual experiment. The relative sensitivity of each *YB-1*$^{+/-}$ ES cell clone was determined by dividing the IC_{50} value for each cell line by the *YB-1*$^{+/+}$ ES cell line IC_{50} value.

Results

Targeted disruption of the *YB-1* gene. The mouse *YB-1* gene, which encodes a 49-kDa protein, is composed of 8 exons, spans more than 16 kb, and is 99% identical to human YB-1. A region of genomic DNA carrying part of two exons and the adjacent intron region, was replaced by a *neo* cassette (Fig. 1A). This region was chosen as the target since it encodes the C-terminal domain of the YB-1 protein, which is essential for protein interaction and nucleoside binding.[26] The resulting construct was electroporated into ES cells, and cells showing increased resistance to both G418 and GANC were selected. The DNAs of resistant clones were digested with restriction enzymes and hybridized with several different probes. Homologous recombinants were characterized by the appearance of a 5.5-kb *Eco*RV fragment with the 5′-internal probe A, and a 10.3-kb *Bgl*II fragment with the 3′-flanking probe B (Fig. 1, B and C). Additional Southern blot analysis using other restriction enzymes confirmed the targeted disruption of one allele of *mouse YB-1* (data not shown). Furthermore, hybridization with the *neo* probe showed that the predicted genomic DNA fragment size is similar in all of these clones. Approximately 4% of G418- and GANC-doubly resistant cells carried the expected structure for the mutated allele.

Decrease in mRNA expression and protein levels in heterozygous *YB-1*$^{+/-}$ ES cells. Northern blot analysis of YB-1 mRNA, using the full-length YB-1 cDNA as a probe, was performed in *YB-1*$^{+/+}$ cells and three different clones of *YB-1*$^{+/-}$ cells. We found that *YB-1*$^{+/-}$ cells contain approximately half the amount of mRNA detected in *YB-1*$^{+/+}$ cells (Fig. 2A). Consistent with this observation, western blot analysis of heterozygously disrupted mutant cells also showed a reduction in YB-1 protein levels. For semi-quantitative analysis, various amounts of cell lysate were applied to the same gel, and we estimated that the protein level of *YB-1*$^{+/-}$ cells was reduced to approximately 50–60% of the wild-type level (Fig. 2B). *YB-1*$^{+/-}$ cells thus established grew normally in ES medium, despite these characteristics. The doubling time of *YB-1*$^{+/+}$ and three clones (1, 2, and 5) of *YB-1*$^{+/-}$ cells were 10.2, 10.0, 9.0, and 10.2 h, respectively (Table 1). Thus, no apparent growth retardation or abnormal cell morphology was found in *YB-1*$^{+/-}$ cells, in spite of the reduced content of YB-1 protein.

Drug, X-ray, and UV irradiation sensitivity of targeted cells to DNA damaging agents. YB-1 has been proposed to be involved in the sensitivity of cells to DNA-damaging agents such as cisplatin and mitomycin C.[15] We therefore explored the role of YB-1 heterozygosity in sensitizing ES cells to a variety of cytotoxic agents using both MTS and clonogenic survival assays. As shown in Table 2, we found that *YB-1*$^{+/-}$ cells are more sensitive to cisplatin and mitomycin C, and moderately more sensitive to etoposide than *YB-1*$^{+/+}$ cells. This enhanced sensitivity was seen in three independently isolated *YB-1*$^{+/-}$ clones (1, 2, and 5), and the depletion of YB-1 was required for drug sensitization. Comparisons made at the IC_{50} dose for cisplatin revealed that *YB-1*$^{+/-}$ cells were approximately 3-fold more sensitive to cisplatin than *YB-1*$^{+/+}$ cells (IC_{50}=20.0 μ*M*). Similarly, comparisons made at the IC_{50} dose for mitomycin C revealed that *YB-1*$^{+/-}$ cells were approximately 5-fold more sensitive to mitomycin C than *YB-1*$^{+/+}$ cells (IC_{50}=9.0 μ*M*). Also, comparisons made at the IC_{50} dose for etoposide revealed that *YB-1*$^{+/-}$ cells showed a moderate level of sensitivity (1.4-

fold), compared with *YB-1*$^{+/+}$ cells (IC_{50}=0.6 μ*M*) (Table 2A). Taken together, the results described above suggest that the concentration of YB-1 appears to correlate inversely with cellular sensitivity to DNA-damaging agents. Clonogenic survival assays were also performed on *YB-1*$^{+/+}$ and *YB-1*$^{+/-}$ cells to determine whether differences observed in MTS survival assays would translate into differences in clonogenicity. We treated cells with a variety of chemotherapeutic drugs, X-ray or UV irradiation and then incubated them for 7 days before counting colonies with greater than 50 cells per colony. This assay provides a longer-term assessment of cell growth than the MTS assay and directly assesses the ability of individual cells to proliferate into viable colonies. We tested the cytotoxicity of cisplatin, mitomycin C, etoposide, X-rays, and UV irradiation against *YB-1*$^{+/+}$ and *YB-1*$^{+/-}$ cells. The dose of agent required to reduce colony formation to 10% (IC_{90}) of that by the control non-treated cells is shown in Table 2B. Consistent with data gained in MTS assays and previous observations in KB cells,[15] *YB-1*$^{+/-}$ cells exhibited greater sensitivity to cisplatin and mitomycin C than *YB-1*$^{+/+}$ cells. The dose-modifying factor for equivalent cell killing (IC_{90}) was approximately 2.0-fold for cisplatin and mitomycin C. In contrast, *YB-1*$^{+/-}$ cells were found to be as sensitive as *YB-1*$^{+/+}$ cells to etoposide, X-ray and UV irradiation (Table 2B, Fig. 3). Our results suggested that the reduction of YB-1 level in ES cells preferentially enhances their sensitivity to DNA cross-linking agents.

No change of p21 levels between YB-1$^{+/+}$ and YB-1$^{+/-}$ cells. Swamynathan *et al.* established DT40 cells, in which one allele of Chk-YB-1b is disrupted.[27] The DT40YB1b (+/−) cells showed multiple abnormalities, such as slow growth rate, increased cell size, increased genomic DNA content, and reduced p21 levels.[27] We found no apparent growth retardation or abnormal cell morphology in *YB-1*$^{+/-}$ cells, in spite of the reduced content of YB-1 protein. We examined whether p21 levels were changed in these wild-type and mutant ES cells. Western blot analysis of heterozygously disrupted mutant cells (YB-1$^{+/-}$) also showed a reduction in YB-1 protein levels, but no change of p21 levels was observed in these wild and mutant ES cells (Fig. 4).

Discussion

To clarify the biological role of YB-1 by modulating the amount of cellular YB-1, cell lines defective in the *YB-1* gene should be useful. In the present study, we have generated *YB-1*$^{+/-}$ cell lines using a gene-targeting techniques. The cell lines established have a sequence alteration in a defined region of one allele of the *YB-1* gene, and display a significant depletion of YB-1 mRNA (approximately 50%). Consistent with the reduction in mRNA transcripts, the protein level of the *YB-1*$^{+/-}$ cells was reduced to approximately 50–60%, compared with that of *YB-1*$^{+/+}$ cells. In this study, insertion of the neomycin (*neo*) cassette resulted in deletion of a 1.8-kb region of the *YB-1* gene, containing a part of exon 5 and all of exon 6. The mutant allele may produce a truncated protein and this protein may function in a dominant-negative manner. We could not detect

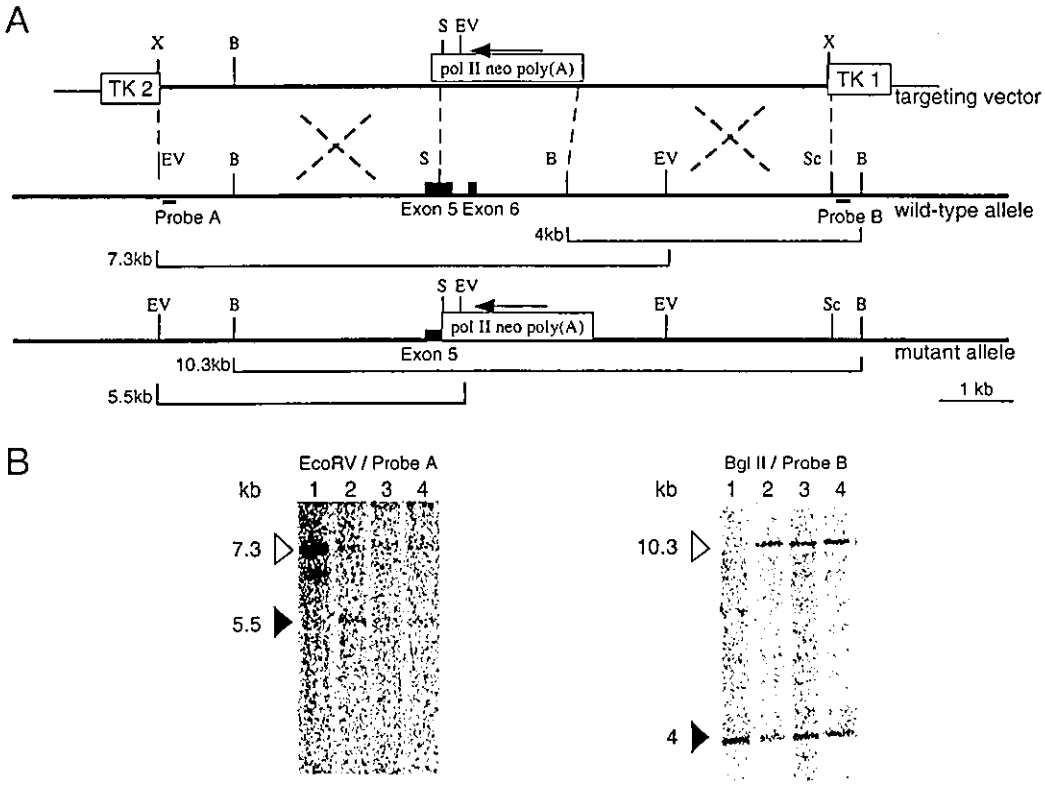

Fig. 1. Targeted disruption of the *mouse YB-1* gene. (A) Configurations of the intact and mutated alleles. The targeting vector carried approximately 8.4 kb of the genomic sequence, within which a part of exon 5 and all of exon 6 was replaced by the *pol*II-*neo*-poly(A) cassette. Restriction enzyme sites are shown; *Xho*I (X), *Bgl*II (B), *Sal*I (S), *Eco*RV (EV), and *Sac*I (Sc). Thick lines indicate the genomic sequence and thin lines represent the bacterial plasmid. The 5′ to 3′ orientation of the *mouse YB-1* gene is left to right, while the 5′ to 3′ orientation of the *pol*II *neo* pA cassette, HSV-1 thymidine kinase gene (TK1) and HSV-2 thymidine kinase gene (TK2) is right to left. Positions of the 5′- and 3′-probes, indicated as probes A and B, respectively, are also shown. (B and C) Southern blot analysis of the DNA isolated from the embryonic stem cell lines. An *Eco*RV digest hybridized with probe A (5′ internal), and a *Bgl*II digest hybridized with probe B (3′ flanking) yielded a wild-type band and a mutant band as indicated. In both cases, genotypes of cells are shown as follows: lane 1, *YB-1*$^{+/+}$; lane 2, clone 1 of *YB-1*$^{+/-}$; lane 3, clone 2 of *YB-1*$^{+/-}$; lane 4, clone 5 of *YB-1*$^{+/-}$.

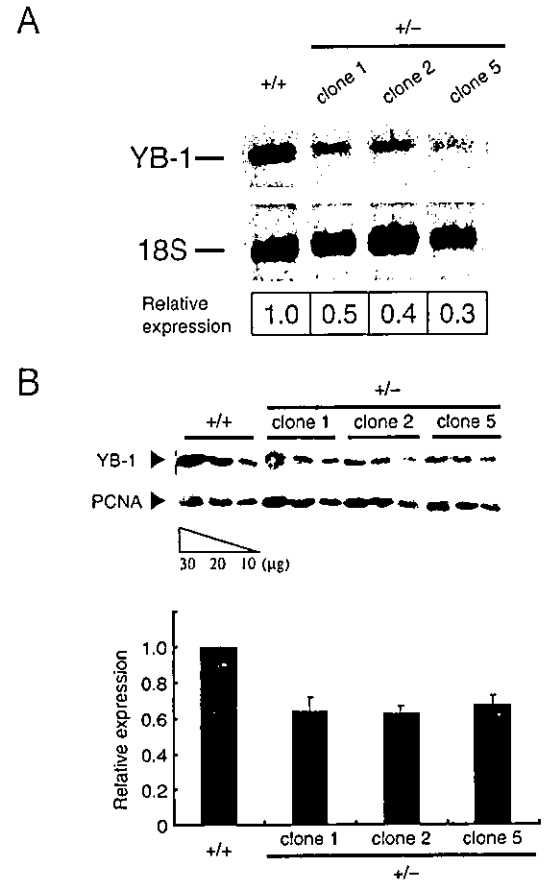

Fig. 2. (A) Northern blot analysis of the *YB-1* mRNA isolated from the germ-line-transmitted embryonic stem cell lines. Total RNA (10 μg) from each cell line was separated on a 1% agarose gel containing 2.2 *M* formaldehyde, transferred to a Hybond N⁺ membrane, and hybridized with ^{32}P-labeled YB-1 cDNA (1060 bp). Relative expression levels of *YB-1* mRNA are presented following normalization to 18S ribosome RNA. (B) Immunoblot analysis of the YB-1 protein isolated from the germ-line-transmitted embryonic stem cell lines. To detect the protein level of YB-1 semi-quantitatively, 30, 20, and 10 μg of total cell lysate were applied to adjacent lanes. The amount of YB-1 in each cell line was quantitated by immunoblot analysis of the same membrane with anti-PCNA antibody and is expressed relative to the amount of PCNA. Relative expression of YB-1 is presented following normalization to PCNA levels.

Table 1. Doubling time of YB-1$^{+/+}$ and YB-1$^{+/-}$ ES cells

Cell lines	Doubling time (h)
YB-1$^{+/+}$	10.2
YB-1$^{+/-}$	
Clone 1	10.0
Clone 2	9.0
Clone 5	10.2

Each value is the mean of duplicate determinations.

the NH_2-terminally truncated form of the YB-1 protein by immunoblotting using an antibody against the NH_2-terminus of YB-1 (data not shown). Although we tried to establish double knockout ES cells (*YB-1*$^{-/-}$) by subsequent culture of heterozygous mutant cells in an elevated concentration of G418, we could not isolate homozygous null mutant ES cells, suggesting that a complete lack of YB-1 may be lethal in ES cells. We have previously shown that YB-1 is directly involved in multidrug-resistance 1 gene activation at the transcriptional level.

Table 2. A. Sensitivity of YB-1$^{+/+}$ and YB-1$^{+/-}$ ES cells to various drugs on MTS assay

Agent	IC_{50}[1] for *YB-1*$^{+/+}$	Relative sensitivity[2] *YB-1*$^{+/-}$		
		Clone 1	Clone 2	Clone 5
Cisplatin (μ*M*)	20.0	0.5	0.3	0.2
Mitomycin C (μ*M*)	9.0	0.3	0.2	0.1
Etoposide (μ*M*)	0.6	1.5	0.5	0.2

B. Sensitivity of YB-1$^{+/+}$ and YB-1$^{+/-}$ ES cells to various drugs on colonogenic assay

Agent	C_{50}[1] for *YB-1*$^{+/+}$	Relative sensitivity[2] *YB-1*$^{+/-}$		
		Clone 1	Clone 2	Clone 5
Cisplatin (μ*M*)	1.5	0.6	0.7	0.4
Mitomycin C (μ*M*)	0.16	0.6	0.6	0.5
Etoposide (μ*M*)	0.07	1.2	1.2	0.9
UV (J/m^2)	3.8	1.1	0.9	0.9
γ-Rays (Gy)	5.4	1.0	1.2	0.8

1) The IC_{50} of *YB-1*$^{+/+}$ and *YB-1*$^{+/-}$ cells for each agent was determined by MTS assay and the IC_{90} was determined by colony formation assays. *2)* The relative sensitivity of each clone of *YB-1*$^{+/-}$ ES cells was determined by dividing the IC_{50} or IC_{90} value for each cell line by that of *YB-1*$^{+/+}$ ES cell line. Values are means derived from two separate experiments.

YB-1 is directly required for basal promoter activation in response to genotoxic stresses, including carcinogens, anticancer agents, and UV irradiation.[7-9] Also, varying levels of expression of the YB-1 protein are associated with many biological phenomena, including cell proliferation and transformation.[5,21,22,28,29] Determining how YB-1 plays a role in biological processes in eukaryotic cells is therefore important. We have shown that YB-1 is located mainly in the cytoplasm, and then accumulates in the nucleus when cells are exposed to genotoxic stress.[16] We have observed that YB-1 is overexpressed in human cancer cells lines that are resistant to cisplatin, and that the amount of YB-1 correlates with the sensitivity of these cells to anti-cancer drugs, cisplatin, mitomycin C and UV irradiation.[15] However, the previously observed inverse correlation between YB-1 levels and drug sensitivity in human cancer cell lines may result from genetic and epigenetic differences unrelated to YB-1 among these cell lines. Single knockout ES cells of various genes, such as O^6-methylguanine-DNA methyltransferase (MGMT) and multiple drug related protein 1 (MRP1), which are associated with DNA repair and drug resistance, respectively, displayed a higher sensitivity to anticancer drugs as compared with their wild-type counterparts.[30,31] In principle, these particular ES cell lines, having a defect in one allele of the *YB-1* gene, could facilitate studies on the biological role of the YB-1 protein.

Cisplatin is widely used in treating a variety of human malignancies. Resistance to this agent is mediated through pleiotropic mechanisms, including decreased drug accumulation, detoxification of the drug, and DNA repair.[32,33] We have also shown that YB-1 levels correlate with sensitivity to cisplatin, suggesting that YB-1 is directly involved in both the cellular response to cisplatin and cisplatin resistance.[15] We therefore examined the sensitivity of the *YB-1*$^{+/-}$ cells to various anticancer drugs, X-rays, and UV irradiation. YB-1$^{+/-}$ cells showed an increased sensitivity to cisplatin and mitomycin C; drugs which induce cross-linking of DNA. Conversely, no dramatic difference in sensitivity to etoposide compared to *YB-1*$^{+/+}$ cells was noted in the MTS assay, or the colony formation assay. Essentially, these results are consistent with the sensitivity levels of YB-1 antisense transfectants, in terms of colony formation.[15]

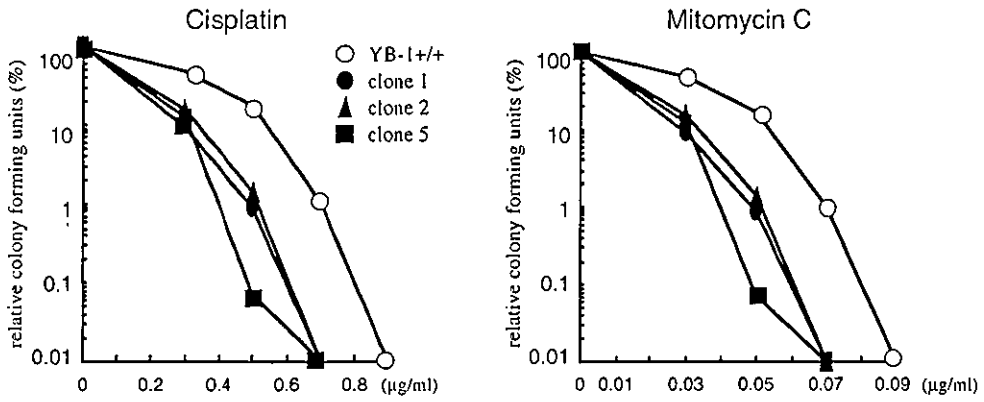

Fig. 3. Dose-response curve to anticancer drugs of *YB-1*$^{+/+}$ and *YB-1*$^{+/-}$ ES cells. Approximately 500 cells were plated on gelatin-coated 6-well plates and incubated in the absence of any drug for 24 h. The cells were then exposed to various concentrations of drugs for 7 days, and the remaining number of colonies was counted; 100% corresponds to the colony number of the same cell line in the absence of any drug. Data points: average values for triplicate dishes.

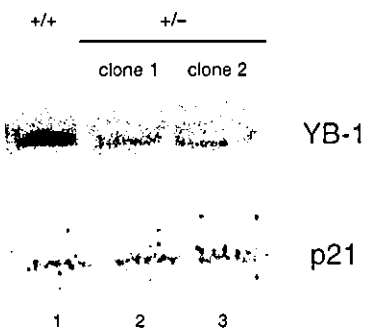

Fig. 4. Immunoblot analysis of the YB-1 and p21 proteins isolated from the germ-line-transmitted embryonic stem cell lines. Total cell lysate (20 μg) was applied to adjacent lanes. In both cases, genotypes of cells are shown as follows: lane 1, *YB-1*$^{+/+}$ ES; lane 2, clone 1 of *YB-1*$^{+/-}$ ES; lane 3, clone 2 of *YB-1*$^{+/-}$ ES.

We consider that the MTS assay can be markedly affected by the rate of cell death, rather than clonogenic survival, and that in turn, can be dependent on the proportion of cells undergoing apoptosis. This may be the reason why we still observed a sensitivity to etoposide in the MTS assay of *YB-1*$^{+/-}$ cells. ES cells with the *YB-1*$^{+/-}$ background had a 60% expression level of YB-1 protein compared to *YB-1*$^{+/+}$ cells. This reduced protein level in *YB-1*$^{+/-}$ cells clearly reflects the sensitivity level of the heterozygous mutant cells, as expected from the findings that stoichiometric amounts of YB-1 protein are needed for sensitivity to cisplatin and mytomicin C. These results indicate that YB-1 is involved in the cellular response to DNA-damaging agents, especially DNA-cross-linking agents. However, in this study no apparent difference in sensitivity to UV irradiation was found between *YB-1*$^{+/-}$ and *YB-1*$^{+/+}$ cells, as compared with the previous study.[15] The IC_{50} dose for UV irradiation of wild-type ES cell was 3.8 (J/m^2), compared to 7.0 (J/m^2) in KB cells. This finding may be a result of the genetic and epigenetic differences between human cancer cell lines and ES cells.

YB-1 has been shown to bind preferentially to cisplatin-modified DNA, apurinic DNA, and RNA containing 8-oxoguanine,[18, 19, 26] suggesting that this protein may bind preferentially to structurally altered DNA.[17] Several nuclear proteins that recognize cisplatin-DNA adducts have been characterized.[32, 34] Among the HMG protein family, HMG1 and HMG2 have been shown to bind specifically to DNA that contains cisplatin-induced intrastrand cross-links[35] and to sensitize cancer cells to cisplatin.[36, 37] Also, IXRI, a yeast protein containing an HMG box, confers sensitivity to cisplatin, though a correlation between the cellular levels of HMG proteins and the repair of damaged DNA has not been demonstrated.[38] It has been established that various repair processes, mainly nucleotide excision repair and mismatch repair, are involved in repair of the cisplatin-induced DNA damage.[39] Cells deficient in DNA repair have been found to be particularly sensitive to cisplatin. Mammalian cells defective in XPF- and ERCC-1, among the proteins involved in nucleotide excision repair, are extremely sensitive to cisplatin.[40] In fact, DNA repair activity has been implicated as a main cause of the resistance of many cell lines to cisplatin. Thus, the cellular sensitivity to cisplatin may be determined by a dynamic interaction between DNA damage recognition processes and DNA repair proteins. We have demonstrated that YB-1 interacts directly with proliferating cell nuclear antigen and p53, which are essential proteins in DNA replication and repair.[18, 20] We have also shown that overexpression of the p53-associated protein p73, involved in DNA repair and apoptosis, increases cellular levels of YB-1,[41] and that YB-1 possesses 3′-5′ DNA exonuclease activity. YB-1 may recognize DNA damaged by a DNA-cross-linking agent, such as cisplatin, and be involved in the process of DNA repair, possibly through interaction with other repair-related proteins.

Recent studies using heterozygous DT40 YB1b (+/−) cells with one copy of the wild-type Chk-YB-1b allele showed a slower rate of growth, abnormal cell morphology, increased cell size, and increased genomic DNA content, compared to wild-type DT40 cells, and it was concluded that YB-1 plays an important role in cell proliferation.[27] In contrast, we found no such apparent growth retardation or abnormal cell morphology of *YB-1*$^{+/-}$ ES cells compared with the wild type. We also found no difference of p21 levels between the two (Fig. 4). This may be due to the following reasons: 1) The level of YB-1 protein in *YB-1*$^{+/-}$ cells was approximately 60% of that of *YB-1*$^{+/+}$ cells and this level of YB-1 protein may be sufficient for the proliferation of *YB-1*$^{+/-}$ cells. 2) DT40 cells were derived from chicken B lymphocytes and do not express p53. Therefore, mouse ES cells may differ greatly from DT40 cells with respect to genetic background, especially regarding the cell cycle and apoptosis control processes. Additional studies are required to determine the differences in phenotype between mouse ES and chicken DT40 cells. Also, the cellular level of YB-1 is associated with tumor growth in ovarian cancers, lung cancers, and breast cancers.[21-23] At present, we have not been able to establish a homozygous null mutant in ES cells. Taken together, these findings suggest that the YB-1 function may be essential for cell viability and proliferation.

In conclusion, we have established YB-1 single knockout cell lines, using gene targeting techniques, and shown that the extent of YB-1 expression correlates with cellular sensitivity to the cytotoxic effects of cisplatin and mitomycin C. YB-1 appears to protect cells or DNA integrity from the toxic insults associated with exposure to DNA-damaging agents. YB-1 is therefore expected to be involved in variety of biological roles, including transcription, cell proliferation, drug resistance, and

DNA repair. To elucidate these physiological roles of the YB-1 protein, establishment of mouse lines defective in *YB-1* genes is in progress. For more definitive studies, designed to evaluate the precise role of the YB-1 protein *in vivo*, the generation of conditional YB-1 mutants may be necessary.

This work was supported by grants from the Ministry of Education, Culture, Sports, Science and Technology of Japan, from the Ministry of Health, Labour and Welfare of Japan, and from Kyushu University Interdisciplinary Programs in Education and Projects in Research Development.

1. Wolffe AP, Tafuri S, Ranjan M, Familari M. The Y-box factors: a family of nucleic acid binding proteins conserved from *Escherichia coli* to man. *New Biol* 1992; 4: 290–8.
2. Makino Y, Ohga T, Toh S, Koike K, Okumura K, Wada M, Kuwano M, Kohno K. Structural and functional analysis of the human Y-box binding protein (YB-1) gene promoter. *Nucleic Acids Res* 1996; 24: 1873–8.
3. Toh S, Nakamura T, Ohga T, Koike K, Uchiumi T, Wada M, Kuwano M, Kohno K. Genomic organization of the human Y-box protein (YB-1) gene. *Gene* 1998; 206: 93–7.
4. Didier DK, Schiffenbauer J, Woulfe SL, Zacheis M, Schwartz BD. Characterization of the cDNA encoding a protein binding to the major histocompatibility complex class II Y box. *Proc Natl Acad Sci USA* 1988; 85: 7322–6.
5. Ladomery M, Sommerville J. A role for Y-box proteins in cell proliferation. *BioEssays* 1995; 17: 9–11.
6. Wolffe AP. Structural and functional properties of the evolutionarily ancient Y-box family of nucleic acid binding proteins. *BioEssays* 1994; 16: 245–51.
7. Uchiumi T, Kohno K, Tanimura H, Matsuo K, Sato S, Uchida Y, Kuwano M. Enhanced expression of the human multidrug resistance 1 gene in response to UV light irradiation. *Cell Growth Differ* 1993; 4: 147–57.
8. Asakuno K, Kohno K, Uchiumi T, Kubo T, Sato S, Isono M, Kuwano M. Involvement of a DNA binding protein, MDR-NF1/YB-1, in human MDR1 gene expression by actinomycin D. *Biochem Biophys Res Commun* 1994; 199: 1428–35.
9. Ohga T, Uchiumi T, Makino Y, Koike K, Wada M, Kuwano M, Kohno K. Direct involvement of the Y-box binding protein YB-1 in genotoxic stress-induced activation of the human multidrug resistance 1 gene. *J Biol Chem* 1998; 273: 5997–6000.
10. Furukawa M, Uchiumi T, Nomoto M, Takano H, Morimoto RI, Naito S, Kuwano M, Kohno K. *J Biol Chem* 1998; 273: 10550–5.
11. Swamynathan SK, Nambiar A, Guntaka RV. Role of single-stranded DNA regions and Y-box proteins in transcriptional regulation of viral and cellular genes. *FASEB J* 1998; 2: 515–22.
12. Matsumoto K, Wolffe AP. Gene regulation by Y-box proteins: coupling control of transcription and translation. *Trends Cell Biol* 1998; 8: 318–23.
13. Sommerville J. Activities of cold-shock domain proteins in translation control. *BioEssays* 1999; 21: 319–25.
14. Tafuri SR, Familari M, Wolffe AP. A mouse Y box protein, MSY1, is associated with paternal mRNA in spermatocytes. *J Biol Chem* 1993; 268: 12213–20.
15. Ohga T, Koike K, No M, Makino Y, Itagaki Y, Tanimoto M, Kuwano M, Kohno, K. Role of the human Y box-binding protein YB-1 in cellular sensitivity to the DNA-damaging agents cisplatin, mitomycin C, and ultraviolet light. *Cancer Res* 1996; 56: 4224–8.
16. Koike K, Uchiumi T, Ohga T, Toh S, Wada M, Kohno K, Kuwano M. Nuclear translocation of the Y-box binding protein by ultraviolet irradiation. *FEBS Lett* 1997; 417: 390–4.
17. Hasegawa SL, Doetsch PW, Hamilton KK, Martin AM, Okenquist SA, Lenz J, Boss JM. DNA binding properties of YB-1 and dbpA: binding to double-stranded, single-stranded, and abasic site containing DNAs. *Nucleic Acids Res* 1991; 19: 4915–20.
18. Ise T, Nagatani G, Imamura T, Kato K, Takano H, Nomoto M, Izumi H, Ohmori H, Okamoto T, Ohga T, Uchiumi T, Kuwano M, Kohno K. Transcription factor Y-box binding protein 1 binds preferentially to cisplatin-modified DNA and interacts with proliferating cell nuclear antigen. *Cancer Res* 1999; 59: 342–6.
19. Hayakawa H, Uchiumi T, Fukuda T, Ashizuka M, Kohno K, Kuwano M, Sekiguchi M. Binding capacity of human YB-1 protein for RNA containing 8-oxoguanine. *Biochemistry* 2002; 41: 12739–44.
20. Okamoto T, Izumi H, Imamura T, Takano H, Ise T, Uchiumi T, Kuwano M, Kohno K. Direct interaction of p53 with the Y-box binding protein, YB-1: a mechanism for regulation of human gene expression. *Oncogene* 2000; 19: 6194–202.
21. Kamura T, Yahata H, Amada S, Ogawa S, Sonoda T, Kobayashi H, Mitsumoto M, Kohno K, Kuwano M, Nakano H. Is nuclear expression of Y box-binding protein-1 a new prognostic factor in ovarian serous adenocarcinoma? *Cancer* 1999; 85: 2450–4.
22. Shibahara K, Sugio K, Osaki T, Uchiumi T, Maehara Y, Kohno K, Yasumoto K, Sugimachi K, Kuwano M. Nuclear expression of the Y-box binding protein, YB-1, as a novel marker of disease progression in non-small cell lung cancer. *Clin Cancer Res* 2001; 7: 3151–5.
23. Janz M, Harbeck N, Dettmar P, Berger U, Schmidt A, Jurchott K, Schmitt M, Royer HD. Y-box factor YB-1 predicts drug resistance and patient outcome in breast cancer independent of clinically relevant tumor biologic factors HER2, uPA and PAI-1. *Int J Cancer* 2001; 97: 278–82.
24. Mansour SL, Thomas KR, Capecchi MR. Disruption of the proto-oncogene int-2 in mouse embryo-derived stem cells: a general strategy for targeting mutations to non-selectable genes. *Nature* 1988; 336: 348–52.
25. Tsuzuki T, Fujii Y, Sakumi K, Tominaga Y, Nakao K, Sekiguchi M, Matsushiro A, Yoshimura Y, Morita T. Targeted disruption of the Rad51 gene leads to lethality in embryonic mice. *Proc Natl Acad Sci USA* 1996; 93: 6236–40.
26. Izumi H, Imamura T, Nagatani G, Ise T, Murakami T, Uramoto H, Torigoe T, Ishiguchi H, Yoshida Y, Nomoto M, Okamoto T, Uchiumi T, Kuwano M, Funa K, Kohno K. Y box-binding protein-1 binds preferentially to single-stranded nucleic acids and exhibits 3′→5′ exonuclease activity. *Nucleic Acids Res* 2001; 29: 1200–7.
27. Swamynathan S, Varma B, Weber K, Guntaka R. Targeted disruption of one allele of the Y-box protein gene, Chk-YB-1b, in DT40 cells results in major defects in cell cycle. *Biochem Biophys Res Commun* 2002; 296: 451–7.
28. Oda Y, Sakamoto A, Shinohara N, Ohga T, Uchiumi T, Kohno K, Tsuneyoshi M, Kuwano M, Iwamoto Y. Nuclear expression of YB-1 protein correlates with P-glycoprotein expression in human osteosarcoma. *Clin Cancer Res* 1998; 4: 2273–7.
29. Shibao K, Takano H, Nakayama Y, Okazaki K, Nagata N, Izumi H, Uchiumi T, Kuwano M, Kohno K, Itoh H. Enhanced coexpression of YB-1 and DNA topoisomerase II alpha genes in human colorectal carcinomas. *Int J Cancer* 1999; 83: 732–7.
30. Lorico A, Rappa G, Flavell RA, Sartorelli AC. Double knockout of the MRP gene leads to increased drug sensitivity *in vitro*. *Cancer Res* 1996; 56: 5351–5.
31. Tominaga Y, Tsuzuki T, Shiraishi A, Kawate H, Sekiguchi M. Alkylation-induced apoptosis of embryonic stem cells in which the gene for DNA-repair, methyltransferase, had been disrupted by gene targeting. *Carcinogenesis* 1997; 18: 889–96.
32. Chu G. Cellular responses to cisplatin. The roles of DNA-binding proteins and DNA repair. *J Biol Chem* 1994; 269: 787–90.
33. Stavrovskaya A. A cellular mechanisms of multidrug resistance of tumor cells. *Biochemistry (Mosc)* 2000; 65: 95–106.
34. Zamble DB, Lippard SJ. Cisplatin and DNA repair in cancer chemotherapy. *Trends Biochem Sci* 1995; 20: 435–9.
35. Timmer-Bosscha H, Mulder NH, de Vries EG. Modulation of *cis*-diamminedichloroplatinum(II) resistance: a review. *Br J Cancer* 1992; 66: 227–38.
36. Arioka H, Nishio K, Ishida T, Fukumoto H, Fukuoka K, Nomoto T, Kurokawa H, Yokote H, Abe S, Saijo N. Enhancement of cisplatin sensitivity in high mobility group 2 cDNA-transfected human lung cancer cells. *Jpn J Cancer Res* 1999; 90: 108–15.
37. He Q, Liang CH, Lippard SJ. Steroid hormones induce HMG1 overexpression and sensitize breast cancer cells to cisplatin and carboplatin. *Proc Natl Acad Sci USA* 2000; 97: 5768–72.
38. Brown SJ, Kellett PJ, Lippard SJ. Ixr1, a yeast protein that binds to platinated DNA and confers sensitivity to cisplatin. *Science* 1993; 261: 603–5.
39. Damia G, Imperatori L, Stefanini M, D'Incalci M. Sensitivity of CHO mutant cell lines with specific defects in nucleotide excision repair to different anti-cancer agents. *Int J Cancer* 1996; 66: 779–83.
40. De Silva IU, McHugh PJ, Clingen PH, Hartley JA. Defects in interstrand cross-link uncoupling do not account for the extreme sensitivity of ERCC1 and XPF cells to cisplatin. *Nucleic Acids Res* 2002; 30: 3848–56.
41. Uramoto H, Izumi H, Ise T, Tada M, Uchiumi T, Kuwano M, Yasumoto K, Funa K, Kohno K. p73 interacts with c-Myc to regulate Y-box-binding protein-1 expression. *J Biol Chem* 2002; 277: 31694–72.

Interleukin-1β Represses *MRP2* Gene Expression Through Inactivation of Interferon Regulatory Factor 3 in HepG2 Cells

Keiji Hisaeda,[1] Akihiko Inokuchi,[1] Takanori Nakamura,[1] Yukihide Iwamoto,[2] Kimitoshi Kohno,[3] Michihiko Kuwano,[4] and Takeshi Uchiumi[1]*

The human multidrug resistance protein 2 (*MRP2*/ABCC2), expressed on the bile canalicular membrane, mediates the multispecific efflux of several organic anions, including conjugates of glucuronate, sulfate, and glutathione. Expression of MRP2 can be altered in response to environmental stimuli such as cholestasis and jaundice. We previously reported that *MRP2* mRNA expression levels are decreased in the nontumorous part of hepatitis C virus-infected human liver tissues, and that inflammatory cytokines inhibit *MRP2* expression in human hepatic (HepG2) cells. We investigated the molecular mechanisms by which inflammatory cytokines modulate *MRP2* gene expression in hepatic cells. Treatment of human hepatic cells with interleukin-1β (IL-1β) or tumor necrosis factor α resulted in a decrease in the protein and mRNA levels of *MRP2*. IL-1β inhibited the transcriptional activity of *MRP2* promoter constructs by 40%, and this inhibition of *MRP2* promoter activity was mediated through the interferon stimulatory response element (ISRE). Electrophoretic mobility shift assays with IL-1β-treated nuclear extracts showed a decrease in the formation of DNA protein complexes, specifically those including interferon regulatory factor 3 (IRF3). Expression of recombinant human IRF3 increased *MRP2* promoter activity. Treatment with a specific extracellular signal-regulated kinase inhibitor relieved IL-1β-induced *MRP2* mRNA downregulation and abrogated the binding of IRF3 to the ISRE element. In conclusion, IL-1β induces downregulation of the *MRP2* gene by inactivating IRF3 binding to ISRE on the *MRP2* promoter in human hepatic cells; this inactivation is accomplished via interference with the extracellular signal-regulated kinase pathway. (HEPATOLOGY 2004;39:1574–1582.)

Transport proteins in the basolateral and canalicular membranes of hepatocytes mediate transport of organic solutes into and from the liver. Biliary elimination of both endogenous compounds and exogenous drugs or poisons is a major physiological self-defense role of various transporters.[1] One of the major transport systems of this type involves the adenosine triphosphate binding cassette (ABC) transporter family. Among the numerous ABC transporters, P-glycoprotein (P-gp/ABCB1) and multidrug resistance protein 2 (*MRP2*/ABCC2) have been shown to mediate transport of cationic and anionic compounds into bile, and bile salt exporting pump (BSEP/ABCB11) has been shown to export bile acids.[2,3] *MRP2* initially was identified as a multispecific organic anion transporter in the canalicular membrane of hepatocytes and was shown to transport a wide range of conjugated compounds, including leukotriene C4, glucuronidase and sulfated molecules, and molecules conjugated to glutathione.[4–6] Inherited defects in *MRP2* result in Dubin-Johnson syndrome, a congenital disease associated with chronic hyperbilirubinemia and

Abbreviations: ABC transporter, adenosine triphosphate binding cassette transporter; P-gp, P-glycoprotein; MRP2, multidrug resistance protein 2; IL, interleukin; IRF3, interferon regulatory factor 3; RANTES, regulated on activation, normal T cell expressed and secreted; HCV, hepatitis C virus; TNFα, tumor necrosis factor α; ERK, extracellular signal-regulated kinase; ISRE, interferon stimulatory response element; PCR, polymerase chain reaction; C/EBP, CCAAT enhancer-binding protein; HNF, hepatocyte nuclear factor; USF, upstream stimulatory factor; EMSA, electrophoretic mobility shift assay; NE, nuclear extract; RXR, retinoid X receptor.

From the Departments of [1]Medical Biochemistry and [2]Orthopedic Surgery, Graduate School of Medical Sciences, Kyushu University, Fukuoka, Japan; the [3]Department of Molecular Biology, University of Occupation and Environmental Health, Fukuoka, Japan; and the [4]Research Center for Innovative Cancer Therapy of the 21st Century COE Program for Medical Science, Kurume University, Fukuoka, Japan.

Received September 30, 2003; accepted February 13, 2004.

Supported by the Second-Term Comprehensive Ten-Year Strategy for Cancer Control from the Ministry of Health and Welfare of Japan and by the Cancer Research Fund from the Ministry of Education, Culture, Sports, Science, and Technology.

Address reprint requests to: Takeshi Uchiumi, MD, PhD, Department of Medical Biochemistry, Graduate School of Medical Sciences, Kyushu University, 3-1-1 Maidashi, Fukuoka 812-8582, Japan. E-mail: uchiumi@biochem1.med.kyushu-u.ac.jp; fax: 81-92-642-6203.

Published online in Wiley InterScience (www.interscience.wiley.com).

DOI 10.1002/hep.20216

jaundice.[7-9] Liver diseases are characterized by disturbances in the hepatobiliary transport of endogenous and exogenous compounds. Hepatic expression of ABC transporters can be influenced by a number of endogenous and environmental factors. Inflammation is induced under various pathological conditions, such as carcinogenesis, cholestasis, and regeneration by partial hepatectomy and by lipopolysaccharides.[10-14] Administrations of inflammatory cytokines interleukin (IL)-6 and IL-1β has been shown to result in a 20% to 60% decrease in the mRNA levels of *MRP2*, organic anion-transporting polypeptide 1, organic anion-transporting polypeptide 2, and bile salt exporting pump in the mouse liver compared with untreated controls.[15] The decreased hepatic expression of these transporters affects the cellular efflux of various physiological compounds, suggesting that these cytokines may play a key role in the hepatic expression of anion transporters in inflammatory cholestasis.[15] Altered expression of the organic anion-transporting polypeptide and Mrp transporters also is expected to influence the pharmacokinetics of various drugs that are transported by these proteins.

The transcription factor interferon regulatory factor 3 (IRF3) is expressed constitutively in many cell types, and its expression is thought to contribute to self-defense from viral infection by inducing type I interferons.[16,17] IRF3 is required for the expression of interferon β and the chemokine regulated on activation, normal T cell expressed and secreted (RANTES) in response to viral infection. In unstimulated cells, IRF3 is present dominantly in the cytoplasm and is phosphorylated in the N terminal domain. After viral infection, the C terminal domain of IRF3 is phosphorylated, leading to dimerization and interaction with the coactivator CBP/p300.[18] This complex is then translocated to the nucleus, where it activates a promoter containing the IRF3 binding site.

We previously compared the expression of ABC transporters between the hepatitis C virus (HCV)-infected and non-HCV-infected liver in patients with hepatic cancers and reported that the expression levels of *MRP2* mRNA and MRP2 protein were decreased significantly and specifically in the nontumorous part of HCV-infected liver tissue.[19] However, the expression levels of other ABC transporters—*MDR1*, *MDR3*, *MRP1*, and *MRP3*—were not significantly different between the HCV-infected and non-HCV-infected liver.[19] We hypothesized that the downregulation of *MRP2* mRNA levels after cytokine treatment occurred primarily at the transcriptional level, and that this reduction in *MRP2* transcription could be the result of alteration in regulatory nuclear transcription factors. We previously characterized regulatory elements in the human *MRP2* promoter in liver cells.[20] In the present study, we show that *MRP2* mRNA transcription decreased 24 hours after IL-1β and tumor necrosis factor α (TNFα) treatment. Nuclear extract treated with IL-1β showed a marked decrease in DNA protein complexes, including IRF3 complexes, and nuclear accumulation of IRF3 was decreased by treatment with IL-1β. The IL-1β–induced *MRP2* mRNA downregulation was relieved by a specific extracellular signal-regulated kinase (ERK) inhibitor. We hypothesize that this inflammatory cytokine-induced downregulation of MRP2 is the result of reductions in both the nuclear accumulation of IRF3 and the binding of IRF3 to interferon stimulatory response element (ISRE), and that these reductions occur via the ERK pathway.

Materials and Methods

Cell Culture. Human hepatoblastoma HepG2 cells were cultured in Dulbecco's modified Eagle's medium (Nissui Seiyaku, Tokyo, Japan) containing 10% fetal calf serum.[19,20] Normal human hepatocytes hNHeps (Sanko Junyaku, Japan) were cultured according to the manufacture's protocol.

Antibodies and Drugs. The antibodies used in these experiments are as follows: MRP2 (M2III-6; Alexis, San Diego, CA), P-gp (C219; Centacor, Malvern, PA), IRF3 (FL425; Santa Cruz Biotech, Santa Cruz, CA), high mobility group protein-I (T-16; Santa Cruz Biotech), and glucose-6-phosphate dehydrogenase (A9521; Sigma-Aldrich, Saint Louis, MO). All IRFs and Sp1 antibodies were purchased from Santa Cruz Biotech. The drugs Actinomycin D, PD98059, SB203580, and SP600125 were purchased from Carbiochem (San Diego, CA).

Preparation of Protein. For whole-cell lysate, cells were washed with ice cold phosphate-buffered saline and solubilized in 0.5 mL of radio-immunoprecipitation assay buffer (50 mM Tris HCl, 150 mM NaCl, 1% Triton X-100, 0.1% SDS, 0.5% deoxycholate, 1 mM phenylmethyl sulfonyl fluoride, and 1 mg/mL trypsin inhibitor) for 30 minutes on ice, then centrifuged at 15,000*g* for 10 minutes at 4°C. For nuclear and cytoplasmic extract, HepG2 and hNHeps were harvested by exposure to trypsin, resuspended in 200 μL of an ice-cold solution containing 10 mM HEPES NaOH (pH 7.9), 10 mM KCl, 0.2 mM ethylenediaminetetraacetic acid (EDTA), 0.2 mM ethylene glycol bis(βaminoethyl ether) (EGTA), 0.5 mM dithiothreitol, and 0.5 mM phenylmethylsulfonyl fluoride, and incubated on ice for 15 minutes. The cells were then lysed by passing 10 times through a 25-gauge needle attached to a 1-mL syringe, and the lysate was centrifuged for 40 seconds in a microcentrifuge. The supernatant was stored for cytoplasmic extract. The nuclear

pellet was resuspended in 100 μL of an ice-cold solution containing 20 mM HEPES NaOH (pH 7.9), 0.4 M NaCl, 0.75 mM spermidine, 0.15 mM spermine, 0.2 mM EDTA, 0.2 mM EGTA, 0.5 mM dithiothreitol, 0.5 mM phenylmethylsulfonyl fluoride, and 25% (vol/vol) glycerol, incubated for 30 minutes on ice with frequent gentle mixing, and then centrifuged for 20 minutes at 4°C in a microcentrifuge to remove insoluble material. The resulting supernatant (nuclear extract) was stored at −80°C.

Northern Blot Analysis. Total RNA was isolated using RNeasy spin columns (Qiagen, Hilden, Germany). 10 μg of total RNA from HepG2 cells was separated on a 1% formaldehyde-agarose gel and transferred to a membrane as described previously.[19] An *MRP2* complementary DNA (cDNA) probe (−28 to 513) was synthesized by polymerase chain reaction (PCR).

Reporter Gene Vector Constructs. The fragments of the 5′ region of the *MRP2* gene were ligated into the SacI and HindIII sites of pGL3-basic (Promega, Madison, WI). All plasmids were analyzed by restriction enzyme digestion, and the promoter inserts were sequenced. Site-directed mutagenesis of ISRE in p-491 MRP2 Luci was performed by a PCR-based method. The promoter sequence was amplified with Taq polymerase, a 5′-primer 491TAGGAGCTCTAGCGACTGATGCCAC and a 3′-primer that introduces a specific mutation into the ISRE region (5′-AGAAGCGAAACT-3′ to 5′-AcgtGCGcgtCT-3′). Amplification was also performed with a 5′-primer that introduces second specific mutation into the ISRE region and a 3′-primer AAGCTTGATTCCTGGACTGCGTC. Mutant constructs of CCAAT enhancer-binding protein β (C/EBPβ), hepatocyte nuclear factor 1 (HNF1), and upstream stimulatory factor (USF) were made using the same method (for C/EBPβ: 5′primer GAACTTTTAACCGCCTGTATTATG; 3′ primer AAGCTTGATTCCTGGACTGCGTC; for HNF1: 5′ primer GGCAAGGTCGGCGATTAAATGG; 3′ primer CCATTTAATCGCCGACCTTGCC; and for USF 5′ primer GGCTTTTTAGTTGTATGTCCATCC; 3′primer GGATGGACATTGTACTAAAAAGCC). A second PCR was then performed with Taq polymerase using the first PCR products as a template. The PCR product was cloned into pGEM-Teasy vector, which was subsequently digested with SacI and HindIII fragments. The fragments were ligated into the SacI and HindIII sites of pGL3-basic (Promega).

Luciferase Assay. HepG2 cells were transfected by the Lipofectamine method as previously described.[21] Briefly, a mixture of 5 μg of Lipofectamine 2000 (Life Technologies, Grand Island, NY), and 1 μg of reporter plasmid was incubated with the cells for 6 hours. Then, fresh medium containing 20 ng/mL IL-1β was added, and the cells were cultured for an additional 24 hours. In separate experiments, 20 μM PD98059 was administered for 30 minutes before IL-1β stimulation. 100 ng of pRL-TK (Promega) was cotransfected as a control for transfection. Luciferase activity was measured using a dual luciferase assay system (Promega). Twenty, 100, or 200 ng of Flag-only vector or Flag-IRF3 vector was cotransfected to investigate the effect of IRF3 function on the MRP2 promoter. Promoter activities are given as the mean ± SD of triplicate transfections. The level of significance of promoter activities in the presence of regular substrates was determined using Student's *t* test.

Electrophoretic Mobility Shift Assay (EMSA). Nuclear extracts were incubated for 30 minutes on ice in a final volume of 20 μL of reaction mixture containing 25 mM HEPES (pH 7.5), 100 mM KCl, 1 mM EDTA, 10% glycerol, 0.7 mM DTT, 10 ng of poly (dIdC), and 1 × 104 cpm of ^{32}P-labeled oligonucleotide probe in the absence or presence of wild-type or mutant (mt) competitors. The samples were electrophoresed on an 8% polyacrylamide gel (polyacrylamide/bisacrylamide ratio, 80:1) in Tris borate buffer. The DNA sequence of the sense strand of the wild-type MRP2ISRE oligonucleotide is GCAGCAGAAGCGAAACTGCAC, and that of the mutant MRP2ISRE is GCAGCAcgtGCGcgtCTGCAC. For supershift experiments, 2 μg of each antibody was added to the reaction mixture.

Results

IL-1β and TNFα Reduced the Expression of the MRP2 Protein and mRNA. We examined whether the MRP2 protein levels were affected by treatment of IL-1β and TNFα in HepG2 cells. Treatment with various doses of IL-1β and TNFα up to 20 ng/mL for 24 hours markedly reduced the MRP2 protein level in a dose-dependent manner, although P-gp levels remained the same. (Fig. 1A). We next examined the effect of IL-1β and TNFα stimulation on *MRP2* mRNA expression levels. *MRP2* mRNA levels were markedly reduced in a dose- and time-dependent manner (Fig. 1B,C). Treatment with IL-1β at 10 ng/mL or TNFα at 1 ng/mL for 24 hours reduced cellular *MRP2* mRNA levels to 40% or less of the levels in the untreated control (Fig. 1B). Treatment for 12 hours or longer with 20 ng/mL IL-1β or TNFα decreased *MRP2* mRNA levels to 30% to 40% of the levels in controls at time 0 (Fig. 1C). We next examined whether IL-1β signaling inhibitors could affect the IL-1β-induced downregulation of *MRP2* gene expression. IL-1β is known to regulate several signal transduction cascades, including the three main kinase cascades, mitogen-acti-

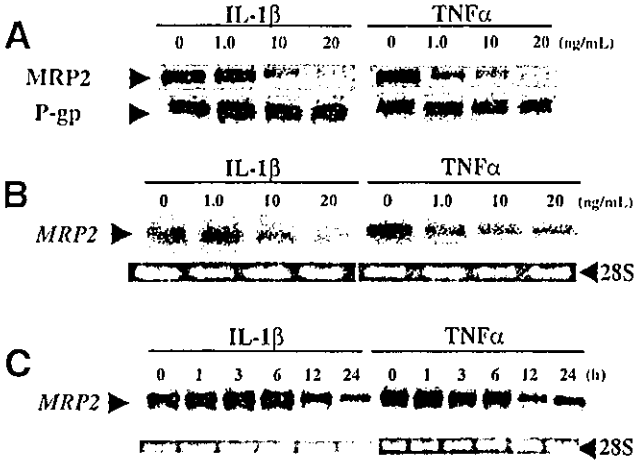

Fig. 1. Alteration of multidrug resistance protein 2 (MRP2) and P-glycoprotein (P-gp)/MDR1 protein and mRNA levels in HepG2 in response to interleukin-1β (IL-1β) or tumor necrosis factor-α (TNFα) administration. (A) For Western blot analysis, 200 μg of protein was loaded, and blots were incubated with an antibody, M2III-6 for MRP2 and C219 for P-gp/MDR1. (B,C) Northern blot analysis. (B) HepG2 cells were treated with the indicated dose of IL-1β (**left**) or TNFα (**right**) for 24 hours. (C) HepG2 cells were treated with 20 ng/mL IL-1β (**left**) or TNFα (**right**) for the indicated time. Ten micrograms total RNA was loaded and hybridized with *MRP2* cDNA. The results were representative of three experiments.

vated protein kinase-ERK, c-Jun NH_2-terminal kinase (JNK), and p38 mitogen-activated protein kinase.[22,23] Coadministration of SB203580 (p38 mitogen-activated protein kinase inhibitor) and SP600125 (JNK inhibitor) with IL-1β had no effect on the IL-1β-mediated downregulation of *MRP2* mRNA levels (Fig. 2, lanes 2, 3, and 5), whereas PD98059 (ERK1/2 inhibitor) almost completely relieved the downregulatory effect of IL-1β (Fig. 2, lanes 2 and 4). There seemed to be no inhibitory effect

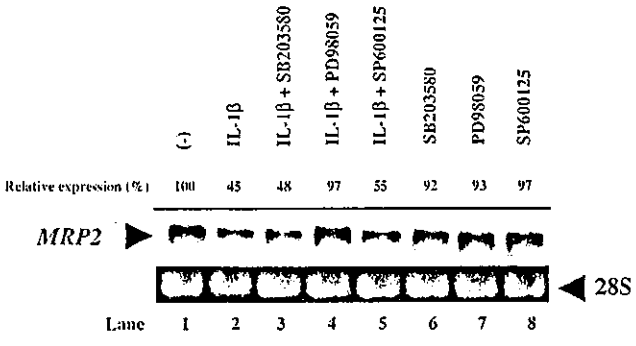

Fig. 2. Extracellular signal-regulated kinase (ERK) pathways were involved in interleukin-1β (IL-1β)-induced *MRP2* downregulation. 20 μM PD98059 (MEK1/2 inhibitor), 25 μM SB203580 (p38 inhibitor), or 20 μM SP600125 (JNK inhibitor) were pretreated for 30 minutes before IL-1β stimulation (20 ng/mL) in HepG2 cells. After 24 hours, total RNA were harvested and hybridized with multidrug resistance protein 2 (MRP2) cDNA. Relative *MRP2* mRNA expression levels are shown, compared with the expression in untreated cells. This result was representative of three experiments.

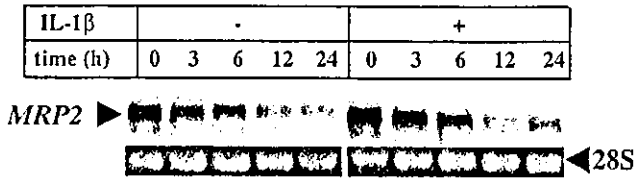

Fig. 3. Rates of *MRP2* mRNA decay. 5 μg/mL actinomycin D was incubated for 30 minutes with HepG2 cells, and interleukin-1β (IL-1β; 20 ng/mL) was administrated for the indicated time. Total RNA was harvested, and 10 μg of RNA was loaded on a 1% formaldehyde-agarose gel and transferred to a membrane. This result was representative of three experiments.

of PD98059 alone on *MRP2* mRNA expression (Fig. 2, lane 7). These results suggest that *MRP2* mRNA downregulation by IL-1β involves the ERK pathway.

To understand how *MRP2* mRNA expression was downregulated by IL-1β, we initially examined whether the stability of *MRP2* mRNA was altered. The *MRP2* mRNA stability was examined, in the absence or presence of IL-1β, by blocking synthesis with 5 μg/mL of actinomycin D (Fig. 3). We observed that *MRP2* mRNA was degraded at similar half-lives of approximately 12 hours under both conditions (Fig. 3), suggesting that IL-1β-induced downregulation of *MRP2* mRNA was not the result of destabilization of mRNA by IL-1β.

Human* MRP2 *Gene Promoter Activity was Inhibited by IL-1β Through an Interferon Stimulatory Response Element at −179/−146bp. We investigated human *MRP2* promoter activity in response to IL-1β administration using a series of 5′-promoter deletion analysis. Deleted promoter fragments were ligated into the reporter gene vector pGL3 basic and were transiently transfected into HepG2 cells. The luciferase activity of the complete series of 5′-deleted *MRP2* promoter constructs is shown in Fig. 4. Compared with p-1659, the luciferase activity decreased to 30% when p-491 was assayed, suggesting that a putative positive cis-element is localized in the −1659/−491 bp region. We also observed an approximately 50% increase in luciferase activity by p-179 as compared with p-491, suggesting that a negative regulatory element is localized in the −491/−179 bp region. Administration of IL-1β reduced *MRP2* promoter activity by 30% to 50% when p-2653, p-1659, p-491, and p-179 were assayed (Fig. 4). However, IL-1β failed to reduce the *MRP2* promoter activity when p-146 and p-21 constructs were assayed. These results suggested that a putative IL-1β response element is located on the −179/−146 region. We identified an ISRE within the −179/−146 region (Fig. 4). To examine whether mutations within the ISRE binding motif affected the downregulation of the *MRP2* promoter activity in response to IL-1β, we performed a mutagenesis analysis of the pro-